AR-009-749

DSTO-TR-0366

DTIC

Evaluation of Innovative NDI Methods for Detection of Widespread Fatigue Damage

P. Khan Sharp,
D.E. Rowlands and G. Clark

DEPARTMENT OF DEFENCE

DEFENCE SCIENCE AND TECHNOLOGY ORGANISATION

DISCLAIMER NOTICE

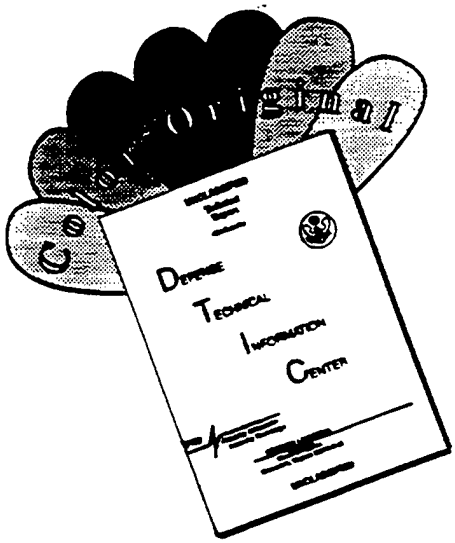

THIS DOCUMENT IS BEST QUALITY AVAILABLE. THE COPY FURNISHED TO DTIC CONTAINED A SIGNIFICANT NUMBER OF COLOR PAGES WHICH DO NOT REPRODUCE LEGIBLY ON BLACK AND WHITE MICROFICHE.

Evaluation of Innovative NDI Methods for Detection of Widespread Fatigue Damage

P. Khan Sharp, D.E. Rowlands and G. Clark

Airframes and Engines Division
Aeronautical and Maritime Research Laboratory

DSTO-TR-0366

ABSTRACT

High-performance high-strength aircraft components such as the F/A-18 FS488 bulkhead can experience catastrophic failure in fatigue tests from very small cracks. At the same time, the efficiency of design methods used for these components results in highly uniform stressing, and a large number of fatigue cracks all growing at approximately the same rate - multi-site cracking. These circumstances place extreme demands upon the use of Non-Destructive Inspection (NDI) methods for finding and characterising defects, and when surface treatments such as peening are also employed to extend service fatigue life, it becomes almost impossible to detect the small crack arrays which are of concern. This report examines and evaluates some novel Non-Destructive Inspection techniques, that may allow numerous small cracks (less than 1 mm) over a large area to be detected. Conventional NDI techniques are also used for comparative purposes.

The novel techniques used are 1) Holographic Interferometry, 2) Structural Integrity Monitor, and 3) Laser Ultrasonics. This report examines the extent to which each technique can locate cracks on a large polished specimen representing part of a bulkhead. Techniques which perform well in this evaluation will be further evaluated on a large peened specimen.

DEPARTMENT OF DEFENCE

DEFENCE SCIENCE AND TECHNOLOGY ORGANISATION

Published by

DSTO Aeronautical and Maritime Research Laboratory
PO Box 4331
Melbourne Victoria 3001

Telephone: (03) 9626 8111
Fax: (03) 9626 8999

AR-009-749
August 1996

APPROVED FOR PUBLIC RELEASE

Evaluation of Innovative NDI Methods for Detection of Widespread Fatigue Damage

Executive Summary

In a fatigue test on a stand-alone F/A-18 FS488 wing carry-through bulkhead, the final failure occurred in a large cross-section, from a fatigue crack size only 6 mm deep. Further evaluation of this bulkhead revealed widespread fatigue cracking. The results confirmed that the bulkhead was a good example of highly efficient design and a classic example of a safe-life component which is expected to perform without inspection. While the widespread use of NDI methods on such a complex component would be difficult, due to its complex shape, surface finish and the small cracks which may be present, it is nevertheless desirable to have available NDI methods which could be used to detect any cracking which might occur in specific critical areas. In that test, conventional NDI techniques were not very successful and the only non-conventional Non-Destructive Inspection (NDI) method used was Acoustic Emission,. While acoustic emission shows promise in the laboratory, there are obstacles preventing its reliable application to flying aircraft.

AED research has already shown how difficult it is to use conventional NDI techniques on peened surfaces due to their rough geometry; at present there are no reliable methods available for detecting the small cracks observed in the bulkhead when those cracks arise at a peened surface. However, there are several "off-the-shelf" NDI techniques that might be useful in this application because they are sensitive primarily to a change in condition, rather than an absolute measurement of crack size. This report examines a number of these innovative NDI techniques including holographic interferometry, "Davey System", and laser ultrasonics and compares their ability to detect cracks on a polished surface. The use of a polished surface enabled the results to be compared with conventional NDI techniques.

The results show that two of the NDI techniques showed promise for detecting small cracks in polished surfaces, and it is proposed that these techniques be further tested to confirm their reliability and detection limits, particularly when used on peened surfaces.

Authors

P. Khan Sharp
Airframes and Engines Division

Khan Sharp, Professional Officer 2. Graduated from Monash University in 1987 having obtained a Materials Engineering Degree with Honours. In 1990 having completed a Masters of Engineering Science he commenced work in the Fatigue and Fracture Detection and Assessment area. Over the past 6 years he has been involved in the metallurgical investigation of aircraft structures and components, fractographic analysis of fatigue surfaces and research into fatigue crack growth and fracture of aircraft materials. He has completed extensive research into novel methods of retarding crack growth and innovative NDI methods. He is presently involved in research tasks on the structural integrity effects of corrosion and fatigue and fracture.

D. E. Rowlands
Airframes and Engines Division

David Rowlands joined DSTO at AMRL in 1988 as a Technical Officer with a background in Metallurgy, Microscopy, and Non-Destructive testing. Since joining AMRL he has worked in the areas of Holographic and Moiré Interferometry, as well as Stress Analysis by Measurement of Thermal Emission. His work has called upon skills in many disciplines such as optics, photography, electronics, experimental design, mechanical testing, as well as data acquisition and analysis.

G. Clark
Airframes and Engines Division

Graham Clark, Principal Research Scientist. Graduated from University of Cambridge in 1972 in Natural Sciences. After completing research for a PhD on the growth of fatigue cracks at notches, undertook post-doctoral research at Cambridge on the detection and growth of crack in submarine pressure vessels. In 1977 he commenced work at DSTO in Maribyrnong, leading research on cracking in thick-walled pressure vessels; which developed a comprehensive fracture control plan for Australian manufactured ordnance and a capability for predicting ordnance fatigue lives. In 1984 he moved to Fishermens Bend, where he established a research program on the damage tolerance of thick carbon-fibre composite materials, involving modelling and experimental investigation of impact damage in aircraft materials. In his present position, he leads tasks which support defect assessment in ADF aircraft, NDI evaluation and fatigue crack growth research. He is also chairperson of the AMRL Accident Investigation Committee.

Contents

1. Introduction

In a fatigue test on a stand-alone F/A-18 FS488 wing carry-through bulkhead, the final failure occurred in a large cross-section, from a fatigue crack size only 6 mm deep. Further evaluation of this bulkhead revealed widespread fatigue cracking. The results confirmed that the bulkhead was a good example of highly efficient design and a classic example of a safe-life component which is expected to achieve its service life without inspection. While the widespread use of NDI methods on such a complex component would be difficult, due to its complex shape, surface finish and the small cracks present, it is nevertheless desirable to have available NDI methods which could be used to detect any cracking which might occur in specific critical areas.

Previous work in AED has shown that conventional ultrasonics, eddy currents and dye penetrants have many problems when used on peened specimens due to the extremely rough surface finish and surface defects. An AED program evaluated NDI techniques that might be used to find small multi-site cracking in a large test specimen. The new NDI techniques selected, according to their individual theories, should overcome the problems in finding surface cracks in a peened surface. The first part of the test program, which is described in this report, has been completed and involves using a large polished specimen, simulating the 6 inch radius of the FS488 bulkhead mouldline flange. This tested the reliability of each NDI technique in finding multisite cracking. The second part of the test will use a peened specimen, similar in configuration to the bulkhead used in service aircraft.

2. Experimental Technique

2.1 General

The aim of the test program was to trial a number of new and innovative NDI techniques. The following NDI techniques were selected for evluation:

1. Laser Ultrasonics,
2. Holographic Interferometry,
3. Structural Integrity Monitor,
4. Standard Ultrasonics,
5. Standard Eddy Current,
6 Visual Inspection with Microwatcher,
7. Fluorescent Dye Penetrant.

While other NDI techniques are available (eg FAST, AC/DC crack gauge etc), they were not included in this trial, because they were not available for the complete test

duration. Due to demand on the 2MN test machine the test was divided into two parts and took over a year to complete. In the initial part of the test approximately 24 programs (1 program = 1 year of simulated flying) of sequence loading were completed, with a further 6 programs completed later. Previous experience with these coupons [2] indicated that cracks should start to appear between 15-25 programs. Therefore, NDI inspections were made every 5 programs till 10 programs, every 2 programs till 16 programs and then every 1 program until the end of the test. The cracks were not grown to specimen failure, so that the test specimen can be used for calibrating other NDI techniques.

At each stage the operator performing each inspection, was only told the total number of programs for recording purposes and was not informed as what other techniques had found. Due to testing time constraints not all the NDI methods were used after every program, except for holographic interferometry and the "Davey System" Structural Integrity Monitor.

2.1.1 Experimental Set up

The coupon tested was machined from a 7050-T7451 plate rolled to 6-inch thickness. A summary of the microstructure and material properties can be found in reference [2]. The coupon dimensions are shown in Figure 1. The coupon surface was polished with 1200 mesh wet-and-dry paper (this was to cause problems with some of the techniques as explained in the results).

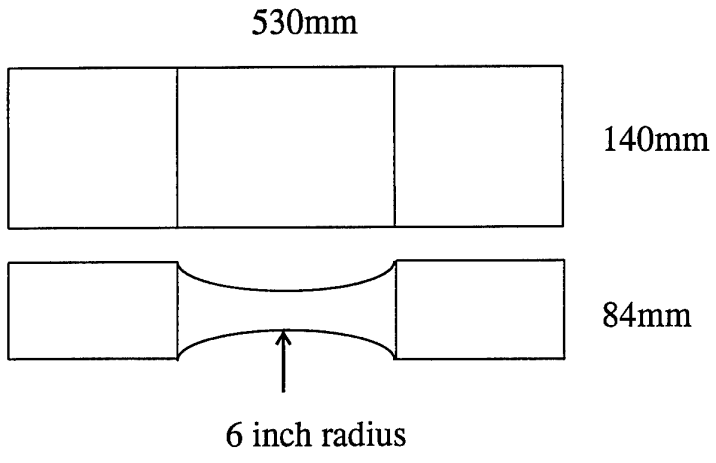

Figure 1: Test coupon dimensions - material aluminium 7050-T7451 plate.

A 2MN hydraulic MTS machine was used to test the coupon. The fatigue test spectrum was IARPO3, which is a FS488 bulkhead spectrum prepared by Canada and comprising some 17332 turning points. The test was stopped after 30 programs due to the confirmed presence of fatigue cracking.

2.1.2 Laser Ultrasonics

The laser ultrasonics was performed by Ship Structures and Materials Division (SSMD) in their experimental rig [3]. Lasers can be used to generate ultrasonic signals in place of piezoelectric transducers, thus allowing rapid non-contact scanning of large areas. Laser ultrasonics is at present primarily a laboratory tool, though it is being developed worldwide with a view to application to aircraft in the longer term.

The laser ultrasonic measurements were performed using laser generation and piezoelectric detection with both generation and detection occurring on the curved surface. Transmission and reflection laser ultrasonic measurements were made at a wide range of generator and detector locations but always with wave propagation parallel to X direction, Figure 2. The centre of the face is defined as co-ordinate (0,0).

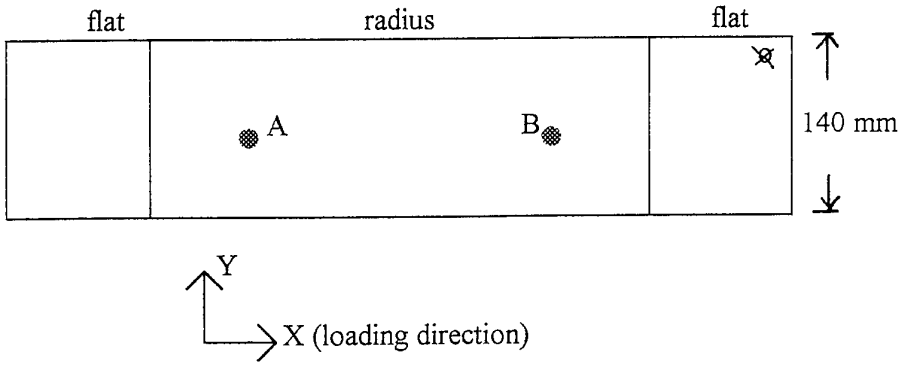

Figure 2: Laser Ultrasonic set-up used at AMRL, positions A and B are the approximate locations used for ultrasonic generation and detection. The centre of the face is defined as co-ordinate (0,0). [3].

2.1.3 Portable Holographic Testing System

The portable holographic testing system was supplied and initially set-up by Bob Clark from the University of NSW, Australian Defence Force Academy (ADFA). The completion of the testing was performed by the authors. The ADFA set-up is technically holographic interferometry of which there are three main types. In this case we are using the most common type, termed double exposure holographic interferometry; the interference is between two optical fields stored on the same plate, each optical field having been recorded at separate times, with the object in slightly different states (ie. different stress state) [4,5]. The authors made a number of changes from the initial set-up due to equipment failure, and attempts to improve image contrast and the number of interference fringes. The holographic set-up [6] is shown in Figure 3.

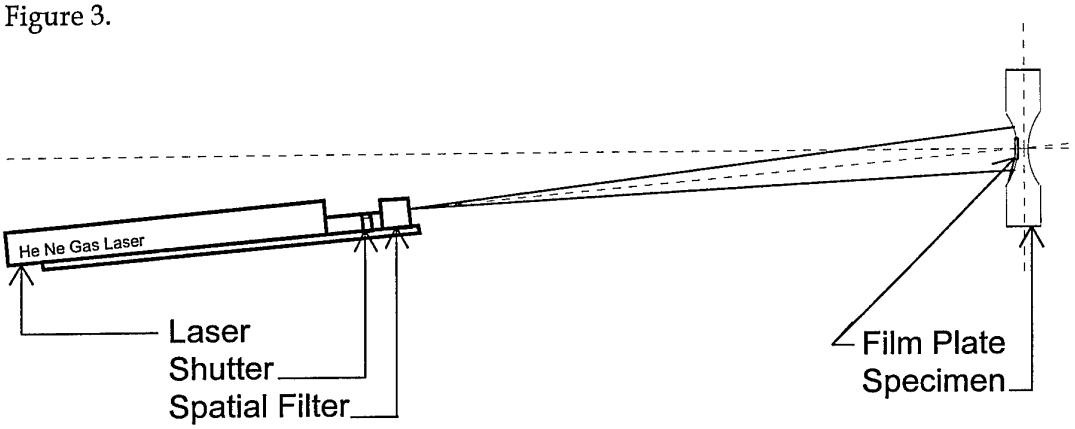

Figure 3: Schematic of interference holographic set-up.

The holographic equipment and its settings were as follows;

Equipment:	ADFA	Melles Griot Helium Neon Gas Laser - Wavelength: 632.8 nm Output: 30mW
		Hughes Series 5000 power supply
		Newport Spatial Filter
		Timer controlled Electromagnetic Shutter
	AED	NEC Helium Neon Gas Laser - Wavelength: 632.8 nm Output: 30mW
Setup:		Distance from spatial filter to specimen = 2.1 m.
		Incident beam to specimen angle = 85°
Holographic Plates:		AGFA - Holotest plates 8E75 HD NAH
		Exposure time = 0.25 to 0.5 seconds

Processing: Development - 5 minutes in Kodak D19
Bleach - 2 to 5 minutes (or until clear), initially with ADFA mixture, latter with "Hariharan's Reversal Bleach"[6].

Two guides were placed on the specimen to locate the holographic plates, just off the surface. The holographic plates had to be mounted and removed in darkness, so a light proof skirt was placed around the test rig with a tube leading to the laser, Figure 4. A darkened room similar to the set-up at ADFA would certainly make this method a lot easier to use. The interference hologram detects any surface displacement differences, therefore for each plate a image is taken at a high and low load to provide the interference fringes. At program 24 (test restart), after some initial trials it was decided to coat the surface with a white lacquer (ARDROX 8901W White Background Lacquer), Figure 5. This provided enhanced contrast and reduced the focused reflection from the specimen surface[5]. Due to the testing environment and the time constraints at AED all the options for creating holographic interferograms were not explored. The system used made it very difficult to determine the correct plate exposure, except by trial and error, therefore, there was a need for numerous changes to be made to determine the optimum conditions; any changes are noted in the report.

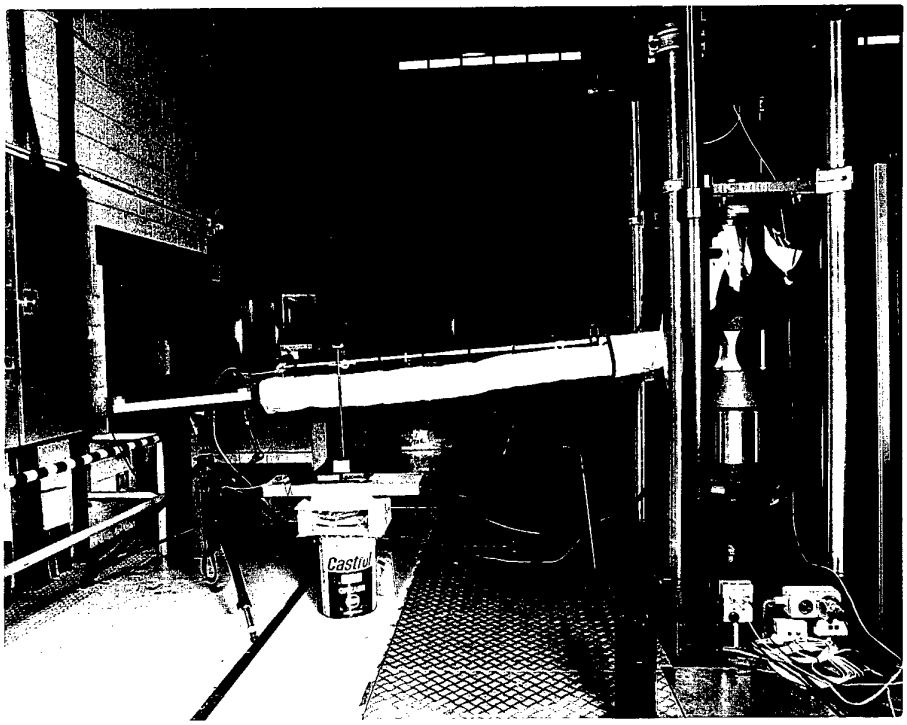

Figure 4: The holographic interferometry set-up showing the skirt surrounding the test machine and the tube leading to the laser.

Figure 5: The surface of the specimen, showing the ARDROX white background lacquer and holographic plate mounts.

One of the major difficulties was found to be interpreting the holographic plates. For the experienced operator there is a large amount of extremely detailed information which, however, can be confusing due to the different interference fringe sets. The reason a fringe pattern is generated and why it can be difficult to reconstruct is set out below.

As detailed by Gordon & Rowlands[7], the fringe pattern is generated by the phase difference $\delta\phi$ between the wavefronts reaching the observer. Referring to Fig. 6, the optical path difference between the source and observer for a small displacement $\underline{d}$ is given by

$$\begin{aligned}\delta\phi &= \underline{d}\,(\underline{k}_2 - \underline{k}_1) \\ &= \underline{d}\,\underline{K}\end{aligned}$$

where $\underline{k}_1$ and $\underline{k}_2$ are the propagation vectors of the incident and reflected light and have a magnitude $|\underline{k}_1| = |\underline{k}_2| = 2\pi/\lambda$, and $\underline{K} = \underline{k}_2 - \underline{k}_1$

$\underline{K}$ is called the sensitivity vector.

When $\delta\phi = \pi, 3\pi, 5\pi...(2n-1)\pi$ destructive interference occurs and dark fringes are generated.

For $\delta\phi = \pi, 2\pi, 4\pi, 6\pi...2n\pi$ constructive interference results in bright fringes.

The sensitivity vector should lie the same direction as the component of displacement of the object that is viewed on reconstruction, and is determined by the geometry of the optical arrangement. Movement of the object normal to the sensitivity vector results in minimum interferometric sensitivity and generates the lowest fringe density.

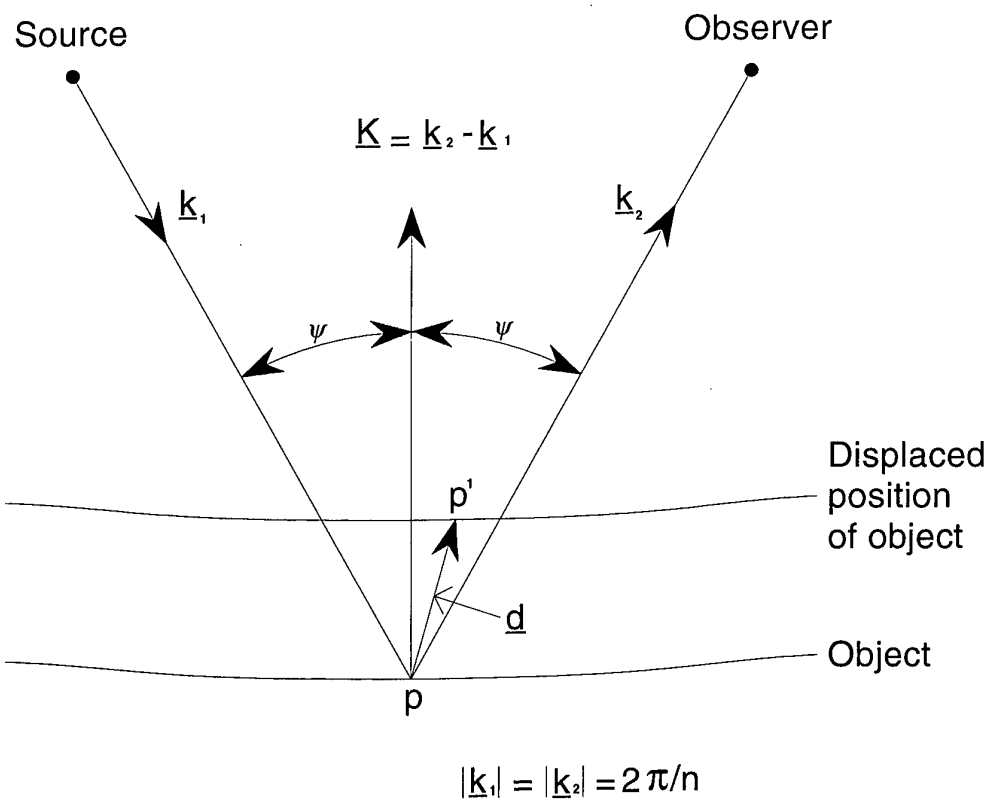

Figure 6: How the holographic fringe pattern is generated.

Some interference fringe sets have to be ignored and others examined, depending on a set of rules. To simplify the interpretation the authors have set up an image system whereby only the useful information is extracted from the hologram. It should be noted that images of the holograms do not fully capture all of the detail that is contained in them. ADFA is developing a capability to transfer the three dimensional information contained in holograms into a two dimensional format, making interpretation simpler. To date the interpretation of holographic plates has proved to be best performed by an experienced operator.

2.1.4 Structural Integrity Monitor "Davey System"

The structural integrity monitor (International Patent Application No. PCT/AU/00235) is an invention by Ken Davey from Structural Monitoring Systems PTY LTD. The technique is a new method for continuously monitoring a structure, whilst in service, to detect the development of flaws. The technique is based on monitoring any change in the pressure difference between a low air pressure and a connected vacuum source [7]. A schematic of the technique, along with how it detects flaws is shown in Figure 7. When a crack joins a low pressure capillary to a vacuum capillary, air leaks across to the vacuum increasing the differential reading. As the crack opens under load more air leaks across to the vacuum giving a higher differential reading; when the load is reduced the crack closes up reducing the reading. The larger the crack the more capillaries it crosses, the higher the differential reading and the more rapid the change, Figure 7.

For our particular case a sensor pad was formed that could be placed over the critical area of the specimen. The initial sensor pad provided by the designer at short notice was made from silicon rubber and had a sensor channel spacing of approximately 1 mm, which proved unsatisfactory (termed Model 1). It was unsatisfactory for two reasons, firstly it could not detect cracks smaller than 1 mm surface length and secondly it was also very difficult to locate a flaw under the sensor pad. There were also complications with the spray adhesive used to bond the sensor pad to the specimen clogging the vacuum capillaries. This gave rise to some further development with the "Davey System".

When the test was restarted (9 months later) some substantial improvements had been made to the sensor pad (termed Model 2) and the overall system. The patch was now made from a photosensitive polymer, reducing the sensor channel spacing to approximately 250 μm, Figure 9. The new sensor pad also came with adhesive backing and a simple method to locate any cracks, horizontally (across the specimen). An alarm and electronic LCD display were also attached to the system to provide a digital readout of the pressure differential, Figure 8, instead of the "left" and "right" gauge system.

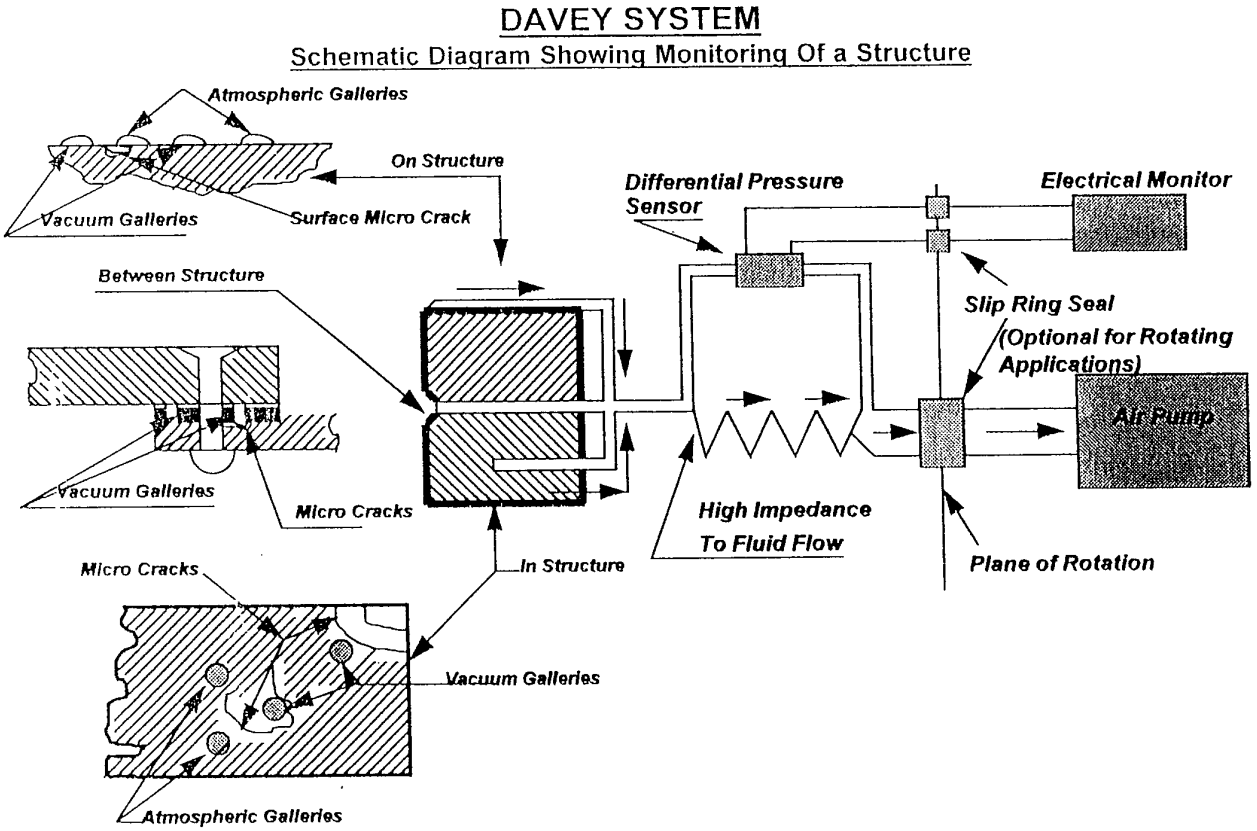

Figure 7: *Schematic of the structural integrity monitor and how it works [7]. A series of parallel galleries (sensor channels) are bonded to the surface to be inspected. The sensor channels alternate between atmospheric pressure and a slight vacuum. When a crack breaches the sensor channel wall, a pressure change occurs as atmospheric air leaks into the vacuum channel.*

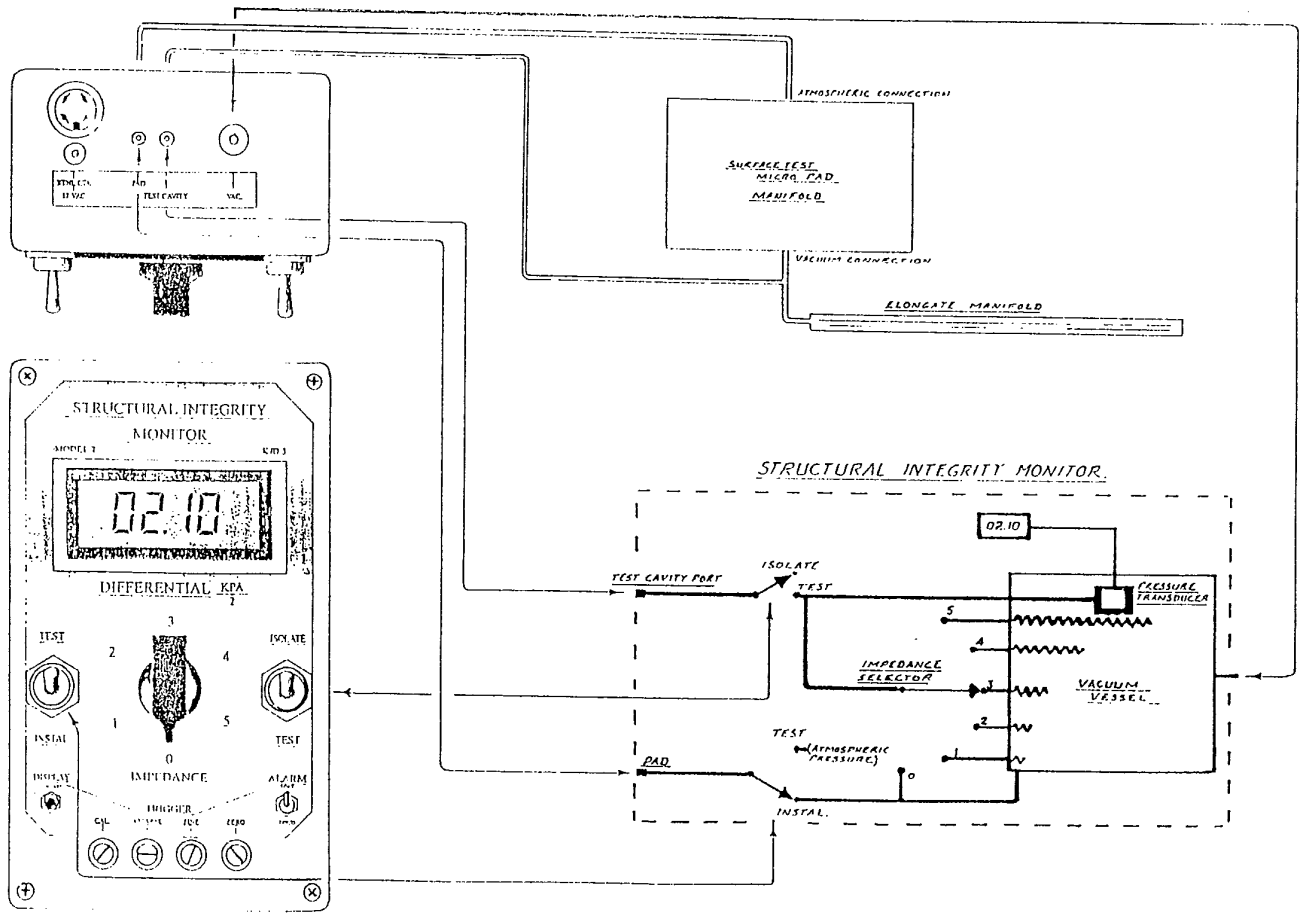

Figure 8: Schematic of the "Davey System" instrumentation, showing the instrument display [7]. this LCD display with alarm was a useful addition to the system, in that it allowed real time results to be displayed.

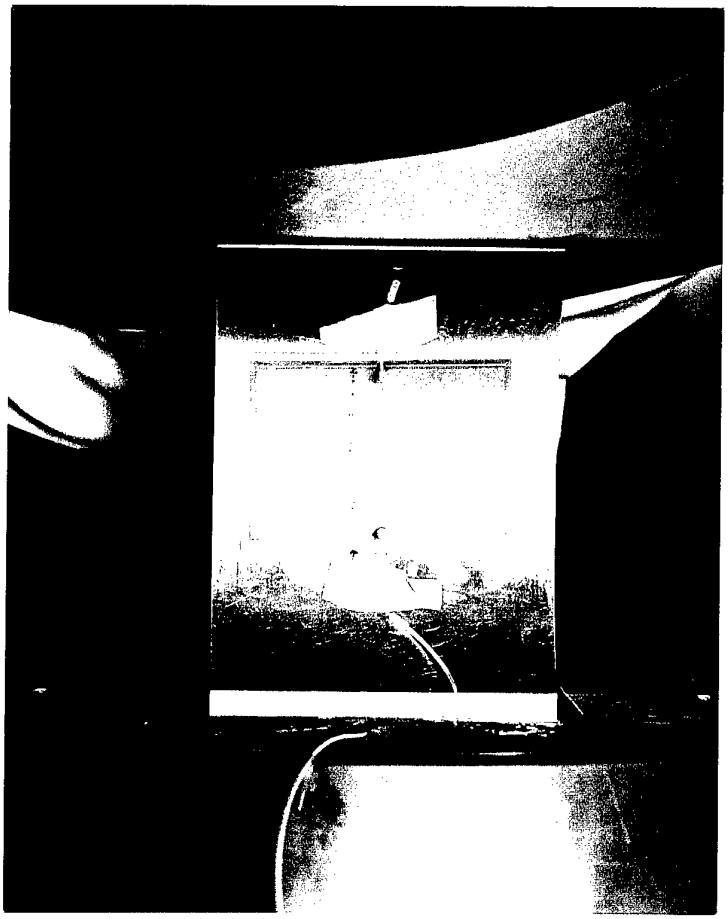

Figure 9: A close up of the structural integrity monitor sensor pad on the specimen.

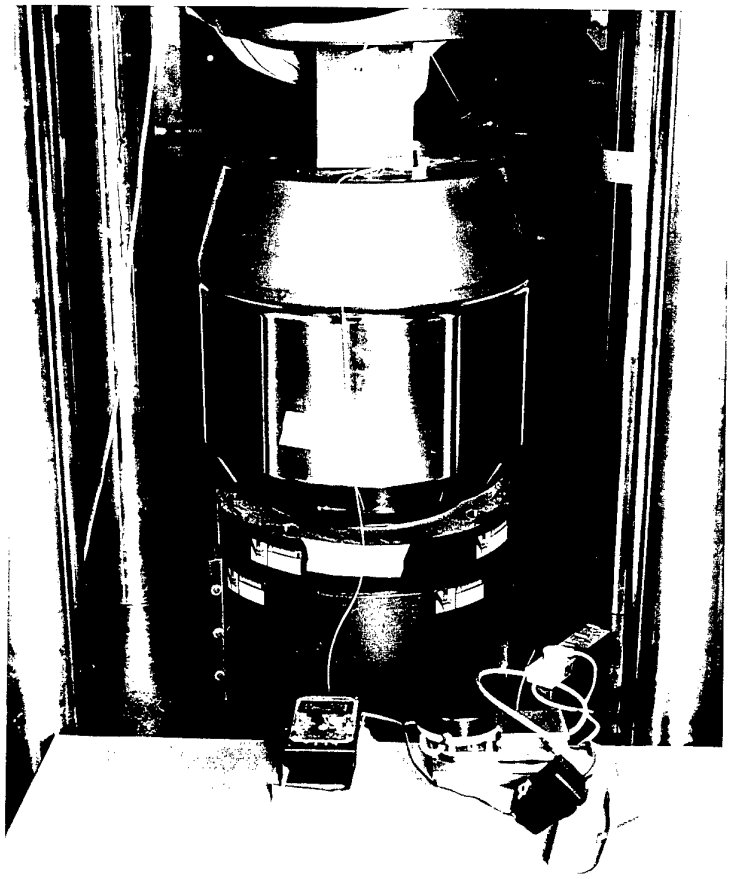

Figure 10: A photograph showing the overall test set-up for the structural integrity monitor. Note the vacuum pump, patent pending, (lower right) and the instrumentation (lower left).

The structural integrity monitor was found to be very simple to use and apply, though care must be taken to ensure that the patch is placed on a clean surface, free from dirt and dust. The patch appears to a very simple way to monitor a large area for defects, though it is still in the initial stages of development.

2.1.5 Standard Eddy Current

Up to program 27 the eddy current machine was a Locator UH, using a 500 kHz type probe. The eddy current system was calibrated to provide 80% full screen height for a 0.5 mm slot. From program 27 onwards a 2 MHz probe was used and calibrated to give a 80% response from a 0.2 mm slot. The inspection was performed by qualified personnel.

2.1.6 Visual Inspection

Extensive video footage of any cracks or crack-like indications was made with a Microwatcher and a "lipstick" miniature video camera. The Microwatcher had a 20x and 50x magnification lens in place. PTFE tape was placed over the focus locater to stop it scratching the specimen surface. Images from the video have been captured onto a Macintosh computer and displayed where appropriate. Video footage of the fluorescent dye penetrant inspection was not very successful with only the larger cracks showing clearly.

2.1.7 Fluorescent Dye Penetrant

A fluorescent dye penetrant inspection was completed at the end of the test to confirm the location of any cracks. The specimen was loaded and Magnaflux ZL-27A penetrant swabbed onto the surface and left for 1 hour. The penetrant was then removed using Magnaflux SKC-NF remover and the specimen unloaded. Magnaflux ZP9E developer was then used to enhance the crack location. The location of each indication was recorded and video footage was taken of the larger indications. Unfortunately the smaller fatigue cracks cannot be seen on the video, due to the low intensity of the UV-light used. While Dye-penetrant can be used with considerable precision on a polished specimen, work on peened surfaces has shown it to be completely unreliable. This is due to the cracked and folded nature of the surface finish after peening [8].

3. Results

The results are set out by program to indicate when each new NDI technique started to indicate cracking or any changes that occurred during testing. Each program is one test spectrum and comprises some 17332 turning points. The specimen was examined after a certain number of programs using a range of NDI techniques and the results noted.

3.1 Program 1

3.1.1 Holographic interferometry

The initial plates were made by Bob Clark from ADFA; the fringe contrast appeared to be reasonably good, with plenty of fringes. For plate No. 1a, exposure time was 0.5 seconds at 50MPa and 250MPa. The first plate had large fringes in the plate from specimen reflections due to the curved polished nature of the surface. For plate No. 1b, exposure time was 0.3 seconds at 50MPa and 250MPa.

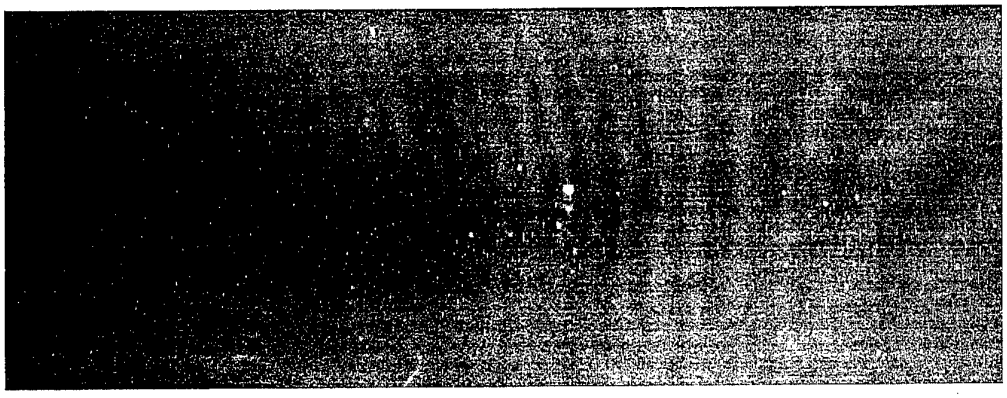

Figure 11: Holographic image from Plate No. 1b.

3.1.2 Structural integrity monitor

The structural integrity monitor (Model 1) was installed on the specimen by the designer and the initial readings taken with zero applied load. With zero load on the specimen the right gauge reading was -83kPa and the left gauge reading was -82kPa, giving a vacuum variation of -1kPa. With a load of 250MPa the gauge readings did not change, giving a differential reading of -1kPa. If a crack was present the differential between the right and left gauges would start to increase with time. The larger the crack the faster the differential would change.

3.1.3 Laser Ultrasonics

The specimen was forwarded to SSMD to be set-up in the test rig. No cracks were found on the specimen. Problems were experienced in reproducibility, arising from poor coupling of the piezoelectric detector to the curved coupon surface. Also optimum conditions for the detection of small cracks could not be achieved due to the low power setting which was needed to stop the laser marking the coupon surface. This problem had not been encountered previously when working with other aluminium alloys. The problem was either due to the surface finish or the nature of the 7050-T7451 plate microstructure.

3.1.4 Conventional NDI techniques

The eddy current and ultrasonic inspections revealed no indication of cracking. A visual inspection both optically and with penetrant revealed no indication of cracking.

3.2 Program 2

3.2.1 Holographic Interferometry

There was no indication of cracking on Plate No. 2, using load levels 50 MPa and 250 MPa, and an exposure time of 1 minute. The long exposure was due to poor alignment of the laser which was rectified, reducing later exposure times to 0.5 seconds.

3.2.2 Structural integrity monitor

There was no change in the differential readings between the right and left hand gauges, indicating that no cracks had been found. With a load of 250MPa, the right gauge reading was -83kPa and the left gauge reading was -82kPa, giving a vacuum variation of -1kPa.

Previous tests had suggested that cracks were unlikely to be observable until around program twenty. Therefore to speed up the test, no other NDI tests were performed on the specimen after the second program until program 5. The structural integrity monitor was left in place on the front of the specimen and the differential reading observed during cycling.

3.3 Program 5

3.3.1 Holographic Interferometry

There was no indication of cracking on Plate No. 3 (load levels 50MPa and 250 MPa, exposure time 0.5 seconds).

Figure 12: Holographic image from plate No3.

3.3.2 Structural integrity monitor

There was no change in the differential readings between the right and left hand gauges, indicating that no cracks had been found. With a load of 250Mpa on the specimen the right gauge reading was -83.5kPa and the left gauge reading was -82kPa, giving a vacuum variation of -1.5kPa.

3.3.3 Conventional NDI techniques

The eddy current, ultrasonic and visual inspections revealed no indication of cracking.

Previous tests had shown that cracks were unlikely to be observable to around program twenty. Therefore to speed up the test, no other NDI tests were performed on the specimen after the fifth program until program 10.

3.4 Program 10

3.4.1 Holographic Interferometry

There was no indication of cracking on Plate No. 4 (load level 50MPa and 250 MPa, exposure time 0.5 seconds). To reduce the number of reflective fringes on the holographic plate, the surface of the specimen was circularly 1200 grit polished. Plate No. 5 had reduced reflective fringes interfering with the desired fringes.

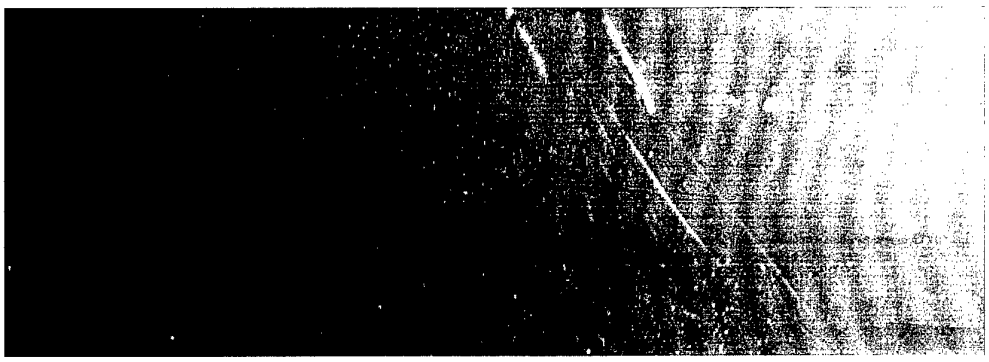

Figure 13: Holographic image of plate No.5.

3.4.2 Structural integrity monitor

There was no change in the differential readings between the right and left hand gauges, indicating that no cracks had been found. With a load of 250MPa on the specimen the right gauge reading was -83kPa and the left gauge reading was -82kPa, giving a vacuum variation of -1kPa.

3.4.3 Conventional NDI techniques

Only the holographic interferometry side (rear side) was inspected with eddy currents and ultrasonics and there was no indication of any cracking being present. Visual examination of both sides did not reveal the presence of any cracking. On the patch side only the area around the patch could be inspected.

Previous tests had shown that cracks were unlikely to be observable to around program twenty. To ensure that the earliest signs of fatigue cracking were detected the five program inspection interval was reduced to two programs.

3.5 Program 12

3.5.1 Holographic Interferometry

Two plates were taken to see if more fringes are developed by the higher load separation. For plate No. 6 the load levels were 50 MPa and 250 MPa, while for plate No. 7 the load levels were 50MPa and 200 MPa, with 0.5 second exposure times. There appeared to be very little difference in the number of fringes between the two load levels.

3.5.2 Structural integrity monitor

There was no change in the differential readings between the right and left hand gauges, indicating that no cracks had been found. With a load of 250Mpa on the specimen the right gauge reading was -82kPa and the left gauge reading was -81kPa, giving a vacuum variation of -1kPa.

3.5.3 Conventional NDI techniques

The eddy current and ultrasonic methods revealed no indication of cracking. A visual inspection with the Microwatcher indicated the possible presence of a 100 μm crack. However, the possible crack was very tight and did not appear to open under load (at 250 MPa). Such a small crack in a large specimen would only open slightly (approx 1-10 μm) which would be undetectable by the Microwatcher.

3.6 Program 14

3.6.1 Holographic Interferometry

Plate No. 8 did not reveal any cracking. The load levels were 50 MPa and 250 MPa, and the exposure time 0.5 seconds.

3.6.2 Structural integrity monitor

There was no change in the differential readings between the right and left hand gauges, indicating that no cracks had been found. With a load of 250MPa on the specimen the right gauge reading was -83kPa and the left gauge reading was -82kPa, giving a vacuum variation of -1kPa.

3.6.3 Laser ultrasonics

There were indications of at least four cracks being present. However, due to the low power input (to minimise specimen damage) the readings were very faint and would have to be compared with later test results to confirm the readings.

Cracks Reported	X (mm) (+/-5 mm)	Y (mm) (+/-5 mm)
(i)	0	0
(ii)	0	-10
(iii)	-3	-10 to -5
(iv)	-9	-10

Figure 14: The location of the potential cracks observed with laser ultrasonics after program 14.

3.6.4 Conventional NDI techniques

The eddy current, ultrasonic and visual inspections revealed no indication of cracking.

Laser ultrasonics provided the first indication of possible cracking, though it could not be confirmed by any of the more traditional methods. Careful optical examination of the surface with a high powered microscope (1000x) was also unable to confirm the presence of any cracking. At this stage the cracks would be extremely small (of the order of 100 μm or less).

3.7 Program 16

3.7.1 Holographic Interferometry

For plate No. 10, exposure time was 0.5 seconds at 50MPa and 250MPa. The fringe contrast was poor, making it very difficult to determine any small distortions in the fringes. More fringes were also needed to improve the sensitivity of the measurement.

3.7.2 Structural integrity monitor

With zero load on the specimen the right gauge reading was -85kPa and the left gauge reading was -82kPa, giving a vacuum variation of -3kPa. The monitor was left to settle for 15 minutes, with final readings of -83kPa and -82kPa, giving a vacuum difference of -1kPa. Table 1 shows the differential readings. There was no indication of cracking.

Table 1: Structural integrity monitor readings after program 20.

Initial Load (MPa)	Final Load (MPa)	Vacuum Reading RHS (kPa)	Vacuum Reading LHS (kPa)	Differential (kPa)
0	0	-85	-82	-3
0	0	-83	-82	-1
0	250	-83	-82	-1

3.7.3 Laser Ultrasonics

This inspection again confirmed the indications of possible cracks at the four sites indicated after program 14. Again the response was weak due to the problems described earlier relating to specimen curvature and use of a low power setting.

3.7.4 Conventional NDI Techniques

The eddy current, ultrasonic and visual inspections revealed no indication of cracking.

Due to the possibility of cracks being present NDI inspections were performed after every program, from program 16 onwards, except for Laser Ultrasonics which was still performed after every two programs.

3.8 Program 17

3.8.1 Holographic Interferometry

For plate No. 11, exposure time was 0.5 seconds at 50MPa and 250MPa. There was no indication of any cracking being present.

3.8.2 Structural integrity monitor

All readings were now taken after a settling time of 15 minutes. With zero load on the specimen the right gauge reading was -83kPa and the left gauge reading was -82kPa, giving a vacuum variation of -1kPa. With a load of 250MPa, there was no change to the differential reading of -1kPa.

3.8.3 Conventional NDI Techniques

The eddy current, ultrasonic and visual inspections revealed no indication of cracking.

3.9 Program 18

3.9.1 Holographic Interferometry

For plate No. 12, the exposure time was 5 seconds at 50MPa and 250MPa. The increase in exposure time from 0.5 seconds to 5 seconds appeared to improve the fringe contrast. More fringes are still needed to improve the sensitivity. There was no indication of any cracking being present.

3.9.2 Structural integrity monitor

With zero load on the specimen the right gauge reading was -83kPa and the left gauge reading was -82kPa, giving a differential reading of -1kPa. With a load of 250MPa, the right gauge reading was -83.5kPa and the left gauge reading -82kPa, giving a differential reading of -1.5kPa.

3.9.3 Laser ultrasonics

The specimen was ungripped and forwarded to the laser ultrasonic laboratory for inspection. This inspection showed indications at (i) and (ii) but determined that the readings at (iii) and (iv) were not cracks but spurious readings due to the specimen curvature.

3.9.4 Conventional NDI Techniques

The eddy current, ultrasonic and visual inspections revealed no indication of cracking.

3.10 Program 19

3.10.1 Holographic Interferometry

For plate No. 13, exposure time was 10 seconds at 50MPa and 250MPa. The increase in exposure time from 5 seconds to 10 seconds was to try and improve the fringe contrast. There was no indication of any cracking.

3.10.2 Structural integrity monitor

The structural integrity monitor readings are shown in Table 2. There was no indication of any cracking being present.

Table 2: Structural integrity monitor readings after program 19.

Initial Load (MPa)	Final Load (MPa)	Vacuum Reading RHS (kPa)	Vacuum Reading LHS (kPa)	Differential (kPa)
0	0	-84	-83	-1
0	250	-84.5	-83	-1.5
250	0	-82.5	-82	-0.5
0	100	-84	-83	-1
0	200	-82.5	-81	-1.5
0	250	-83.5	-82	-1.5

3.10.3 Conventional NDI techniques

The eddy current, ultrasonic and visual inspections revealed no indication of cracking.

3.11 Program 20

3.11.1 Holographic Interferometry

For plate No. 14, exposure time was 15 seconds at 50MPa and 250MPa. The increase in exposure time from 10 seconds to 15 seconds was to try and improve the fringe contrast. The plate was over exposed with no holographic information recorded.

3.11.2 Structural integrity monitor

The structural integrity monitor readings are shown in Table 3. There was no indication of any cracking being present.

Table 3: Structural integrity monitor readings after program 20.

Initial Load (MPa)	Final Load (MPa)	Vacuum Reading RHS (kPa)	Vacuum Reading LHS (kPa)	Differential (kPa)
0	0	-84	-83	-1
0	250	-81.5	-80.5	-1
250	0	-84	-83	-1

3.11.3 Conventional NDI techniques

The eddy current and ultrasonic inspections revealed no indication of cracking. A detailed examination of the specimen surface on a Reichert MEF3 Optical Microscope indicated that there might possibly be a number of 20-40 μm long cracks. These potential cracks were extremely tight and it was not possible to confirm them as fatigue cracks. The microwatcher did not have sufficient image quality to determine if the potential cracks were opening under load. The location of these potential cracks did not match the laser ultrasonics potential crack locations.

3.12 Program 21

3.12.1 Holographic Interferometry

Plate No. 15, exposure time was 15 seconds at 50MPa and 250MPa. There was no indication of any cracking.

3.12.2 Structural integrity monitor

The structural integrity monitor readings are shown in Table 4. There was no indication of any cracking being present.

Table 4: Structural integrity monitor readings after program 21.

Initial Load (MPa)	Final Load (MPa)	Vacuum Reading RHS (kPa)	Vacuum Reading LHS (kPa)	Differential (kPa)
0	0	-83	-75	-8#
0	0	-85	-85	0
0	250	-83	-84.5	1.5
250	0	-85	-84	-1

Leak around edges of patch, once patch was pressed down the readings returned to normal.

3.13 Program 22

3.13.1 Holographic Interferometry

For plate No. 16, exposure time was 15 seconds at 50MPa and 250MPa. The plate was overexposed with no holographic information recorded.

3.13.2 Structural integrity monitor

The structural integrity monitor readings are shown in Table 5. There was no indication of any cracking being present.

Table 5: Structural integrity monitor readings after program 22.

Initial Load (MPa)	Final Load (MPa)	Vacuum Reading RHS (kPa)	Vacuum Reading LHS (kPa)	Differential (kPa)
0	0	-83.5	-83	-0.5
0	250	-85	-84	-1
250	0	-85	-83	-2

3.14 Program 23

3.14.1 Holographic Interferometry

For plate No. 17, exposure time was 15 seconds at 50MPa and 250MPa. There was no indication of any cracking.

3.14.2 Structural integrity monitor

The structural integrity monitor readings are shown in Table 6. There was no indication of any cracking being present.

Table 6: Structural integrity monitor readings after program 23.

Initial Load (MPa)	Final Load (MPa)	Vacuum Reading RHS (kPa)	Vacuum Reading LHS (kPa)	Differential (kPa)
0	0	-83.5	-83	-0.5
0	250	-85	-83	-2
250	0	-85	-83	-2

3.14.3 Conventional NDI techniques

The eddy current, ultrasonic and visual examinations did not reveal any cracking. The possible cracks observed microscopically after program twenty were not observed, by any of the NDI techniques.

3.15 Program 23+13493 TP

During program 24, a power failure caused the test machine to shut down after 13493 turning points. The specimen had therefore completed 23 programs 13493 turning points when it was removed from the test machine.

3.15.1 Holographic Interferometry

For plate No. 18, exposure time was 15 seconds at 50MPa and 250MPa. There was no indication of any cracking.

3.15.2 Structural integrity monitor

With zero load on the specimen the right gauge reading was -83kPa and the left gauge reading was -82kPa, giving a differential reading of -1kPa. With a load of 250MPa, the right gauge reading was -83.5kPa and the left gauge reading -82kPa, giving a differential reading of -1.5kPa.

3.15.3 Laser ultrasonics

The only indications of cracking after program 23+13493tp, were sites (i) and (ii), the other possible having been confirmed as false positive indications. The lack of apparent development of indications (i) and (ii) between programs 14 and 23+, and the lack of development of any other indications in this period indicates non crack-like behaviour. However, as indicated earlier, it was necessary to continue the test until cracks grew to visible length in order to confirm/reject indications confidently.

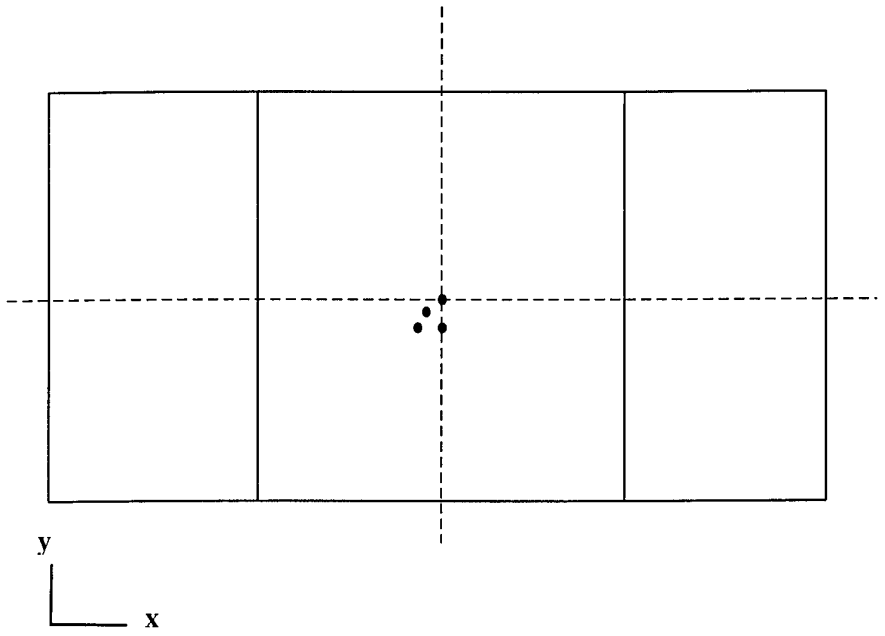

Figure 15: Location of possible cracks detected with laser ultrasonics. These possible crack locations could not be confirmed by any other method.

3.15.4 Conventional NDI techniques

The eddy current, ultrasonic and visual examinations did not reveal any cracking. The specimen was again placed on the MEF3 optical microscope, and the potential cracks observed after program twenty still appear to be between 20-40 μm in length.

The first part of the test was completed and the specimen removed from the test rig due to demand for the 2MN test machine. The specimen was then reinstalled into the test machine after a period of 9 months. The specimen was carefully protected and placed in a constant environment for this period.

3.16 Program 24 - Test Restart

The test was now restarted, with significant improvements to both the holographic interferometry and structural integrity monitor (Model 2) . The changes were made in response to the results from the first part of the test. While the test was not designed to develop NDI techniques, the 9 month delay was beneficial to all techniques in improving their capabilities. Due to the power failure after program 23, program 24 was therefore restarted, meaning that 13493 turning points should be added to each program number from program 24 onwards. Due to time constraints, laser ultrasonics was not performed after every two programs, but was performed when the test was completed.

3.16.1 Holographic Interferometry

In an effort to overcome some of the earlier problems with the low number of interference fringes and the poor fringe contrast the authors made a number of modifications to the initial ADFA process, Table 7. First, a white background was used; this worked extremely well in enhancing the fringe contrast. Secondly, some plates were taken low load-high load and high load-low load to try and improve the number of fringes. It was found that by exposing the plate first under high load and then at low load there was a distinct improvement in the contrast and number of fringes present.

Table 7: Holographic test plates to determine optimum conditions.

Plate No.	Exposure No.	Stress Min (MPa)	Stress Max (MPa)	Load Sequence	Background	Exposure Time (seconds)
1	1	50	200	High - Low	None	15/15
2	2	50	200	Low - High	None	30/30
3	3	50	200	Low - High	White	30/30
4	4	50	200	High - Low	White	15/15
5	5	50	200	High - Low	White	10/10
6	6	50	200	High - Low	White	10/10

At the completion of these tests, all subsequent holograms were taken with a white background under high load - low load sequence.

3.16.2 Structural integrity monitor

The structural integrity monitor now has one digital readout which provides the differential. As before the larger the differential reading and the quicker it changes the larger the crack. The differential had an average reading of 9.10; this was regarded as the base line because the reading did not vary with load or time. The monitor was left to stabilise for 2 hours with very little change. The specimen was also loaded up to 200MPa with little variation in the reading. There was no indication of any cracks being present at this stage.

3.17 Program 25

3.17.1 Holographic Interferometry

With some adjustments to the set-up (associated with shutter problems), the exposure times were reduced from 10 seconds to 2.5 seconds, Table 8.

Table 8: Holographic test plates to improve test conditions

Plate No.	Exposure No.	Stress Min (MPa)	Stress Max (MPa)	Exposure Time (seconds)	Comments
7	7	50	200	7.5/7.5	Bracket exposures
8	8	50	200	15/15	Bracket exposures
9	9	50	200	10/10	Shutter problems
10	10	50	20	15/15	Shutter problems
11	11	50	200	20/20	Shutter problems
12	12	50	200	5/5	Fix shutter
13	13	50	200	2.5/2.5	Laser beam angle

There was no indication of any cracking being present on any of the holographic plates. The conditions had improved significantly, with plenty of contrast and numerous fringes on the plates.

3.17.2 Structural integrity monitor

The differential reading was again stable at around 9.10, however, when the specimen was loaded to 200MPa the differential reading went up to 10.27. On unloading back to zero the reading slowly dropped back to approximately 9.10. This was the first indication that a crack was present on the front face of the specimen. The lag in the reading was very noticeable with small differential variations, the reading taking up to 4 minutes to stabilise at the higher load level[1].

Table 9: Check of the lag time in the structural integrity monitor instrument.

First Load (MPa)	Differential Reading	Next Load (MPa)	Differential Reading	Time to steady state (minutes)
0	9.13	150	9.27	2
0	9.01	150	9.25	2
150	9.30	200	10.27	2
200	10.24	150	9.49	6
200	10.10	50	9.38	6

[1] It is understood that the designer is presently modifying the monitor to reduce this lag time to a more acceptable time.

The crack was detected under the patch, though the lag in the system made it difficult to locate the crack precisely. The patch was not removed to confirm the presence of a crack by conventional NDI techniques.

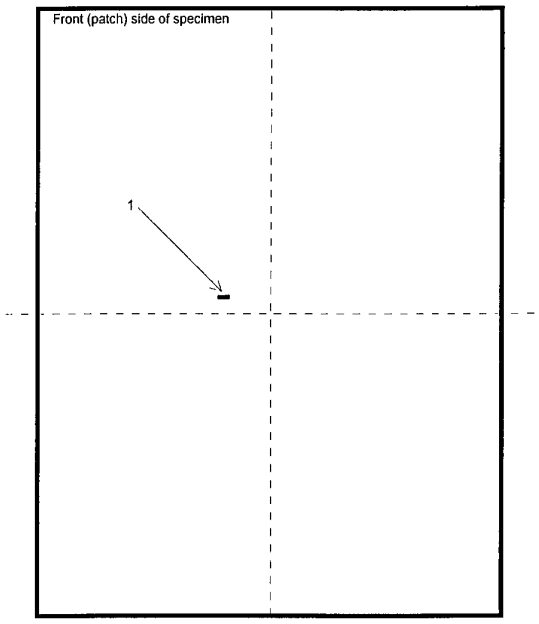

Figure 16: The suspected location of the crack detected, this location was not precise due to the lag in the instrument system.

3.18 Program 26

3.18.1 Holographic interferometry

The power supply to the ADFA laser failed making the ADFA laser inoperative. Fortunately the instrument could be replaced by a similar laser (power and wavelength).

For plate No. 15, the exposure time was 0.5 seconds at 50MPa and 250MPa. There was significant fringe distortion identifying cracks in three locations, Figure 17, two cracks are toward the left edge of the specimen and one crack left of centre, Figure 18. Another two small crack indications can be observed in the distorted fringes on the plate.

Table 10: Holographic test plates to improve test conditions.

Plate No.	Exposure No.	Stress Min (MPa)	Stress Max (MPa)	Exposure Time (seconds)
14	14	50	200	1/1
15	15	50	200	0.5/0.5

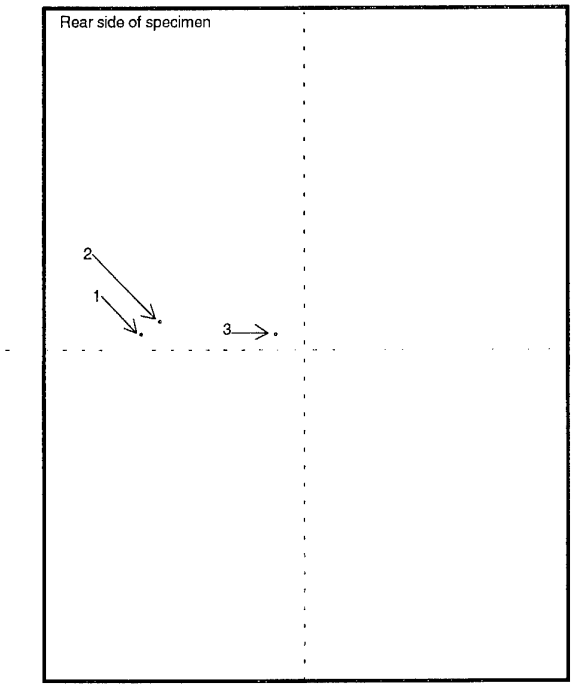

Figure 17: A schematic of the location of the three cracks detected.

Figure 18: An image of the three cracks, showing the distortion in the fringes.

3.18.2 Structural integrity monitor

The differential reading was again stable at around 9.10, however, when the specimen was loaded to 200MPa the differential reading went up to 13.63. On unloading back to zero the reading slowly dropped back to approximately 9.10.

Table 11: Structural integrity monitor readings after program 26.

First Load (MPa)	Differential Reading	Next Load (MPa)	Differential Reading	Time to steady state (minutes)
cyclic	10.26	cyclic	10.80	
0	9.28	200	13.63	2
0	9.17	150	10.76	2
150	10.76	150	10.82	Hold

Three possible microcracks were located approximately 56 mm, 62 mm and 75 mm from the left hand edge of the specimen. It was not possible to locate the cracks vertically under the patch.

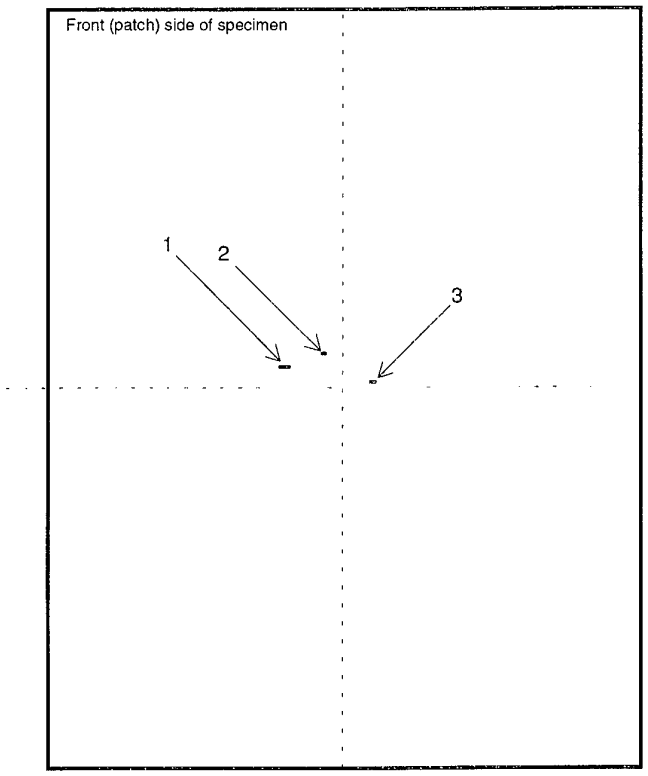

Figure 19: A schematic of the location of the three cracks detected by the structural integrity monitor (Model 2).

3.19 Program 27

3.19.1 Holographic Interferometry

A number of cracks were clearly observable, Figure 20. On Plate No. 16, there is a prominent crack just to the right of centre, Figure 21, along with the cracks observed in program 26. Plate No. 17 clearly shows the three cracks observed in program 26, with indications below the two on the left hand side of the specimen, Figure 22.

Table 12: Holographic plate tests.

Plate No.	Exposure No.	Stress Min (MPa)	Stress Max (MPa)	Exposure Time (seconds)
16	16	50	200	0.5/0.5
17	17	50	200	0.5/0.5
18	18	50	200	0.5/0.5
19	19	50	200	0.5/0.5
20	20	50	130	0.5/0.5

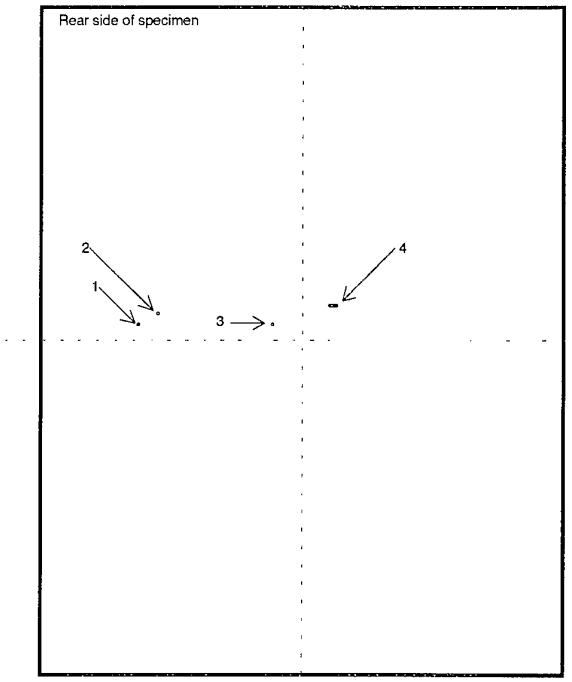

Figure 20: A schematic of the locations of the four cracks now found. Three cracks were found after program 26 (No's 1,2,3) and a new large crack was found at location No. 4.

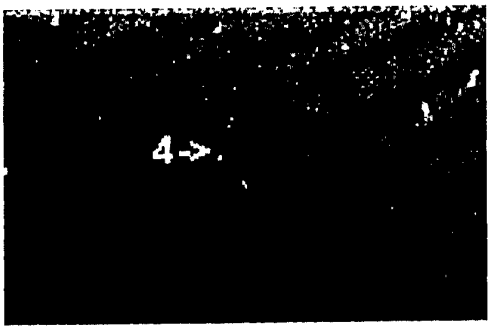

Figure 21: A holographic image of the large crack located at No; 4.

Figure 22: A holographic image of the three cracks, observed after program 26.

3.19.2 Structural integrity monitor

The differential reading was again stable at around 9.28, however, when the specimen was loaded to 200MPa the differential reading went up to 23.35. On unloading back to zero the reading slowly dropped back to approximately 9.58. The static loading triggered the monitor alarm which had been set for a differential reading of 20. The increase in the differential reading from 13.63 (program 26) to 23.53 in program 27 is an indication of the presence of a large crack or cracks.

Table 13: Structural integrity monitor readings.

First Load (MPa)	Differential Reading	Next Load (MPa)	Differential Reading	Time to steady state (minutes)
Cyclic	10.26	Cyclic	11.49	
0	9.58	200	21.08	2
200	21.08	0	9.60	4
0	8.30	0	8.30	Ungripped
0	8.30	100	12.66	4
100	12.65	200	22.19	4
0	9.30	200	23.35	2

The crack was located approximately 58 mm from the left hand edge. Though there were still indications at approximately 65 mm and 70 mm the signal was being dominated by the crack located 58 mm from the edge. This indicates that there was one large crack at 58 mm and two small cracks at 65 mm and 70 mm. The fact that the zero load differential reading was slowly creeping up also indicated that a crack was present.

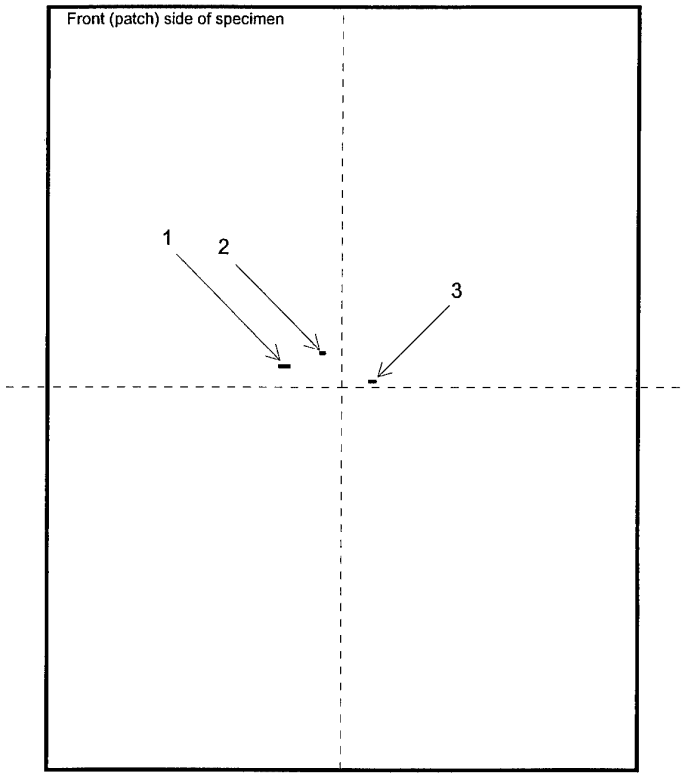

Figure 23: A schematic of the location of the three cracks detected by the structural integrity monitor (Model 2). Crack No.1 was large and starting to swamp the signal from cracks No. 2 and No. 3.

3.20 Program 28

3.20.1 Holographic Interferometry

Plate No. 22 clearly shows the major four cracks observed from program 26 onwards, Figure 24. There was also a possible crack indication left of centre just below the middle of the specimen.

Table 14: Holographic plate test conditions.

Plate No.	Exposure No.	Stress Min (MPa)	Stress Max (MPa)	Exposure Time (seconds)
21	21	50	200	0.5/0.5
22	22	50	200	0.5/0.5

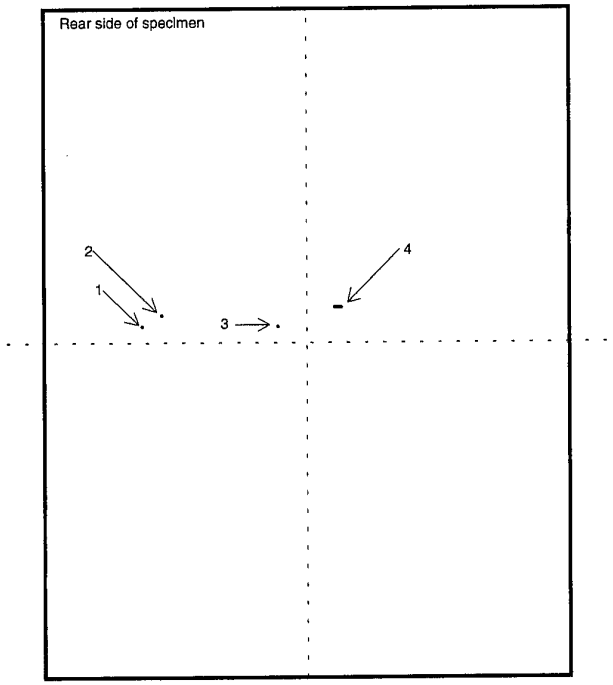

Figure 24: A schematic of the location of the four cracks detected with holographic interferometry.

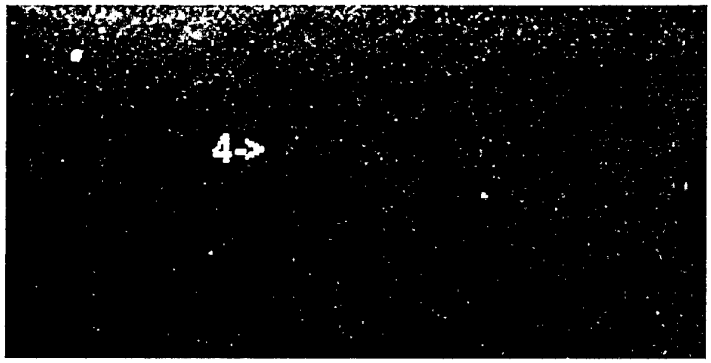

Figure 25: An image of the large crack No. 4. The crack is growing larger and disturbing more fringes..

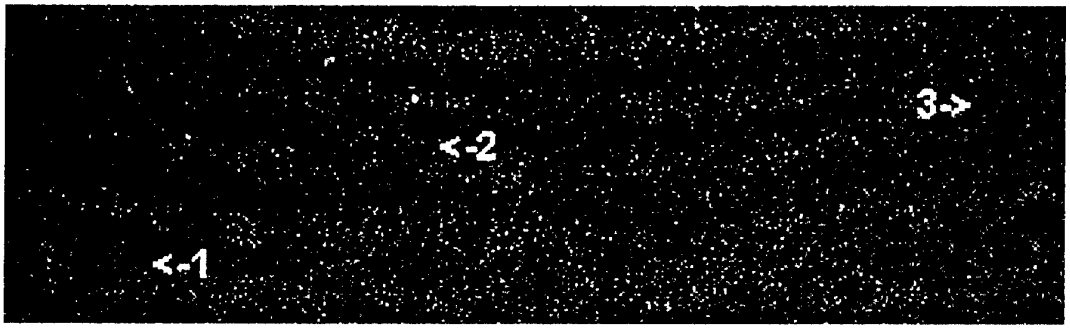

Figure 26: The other three cracks located after program 28.

3.20.2 Structural integrity monitor

The monitor alarm was set at 40.00 (arbitrary point above spectrum 27 maximum based on K. Davey experience). The alarm was triggered during all static loading sequences, though it was not activated while under cyclic loading. The structural integrity monitor readings are listed in Table 15. The increase in the differential reading from 23.35 (program 27) to 42.60 in program 28 was a clear indication of a rapidly growing crack or cracks.

Table 15: Structural integrity monitor readings after program 28.

First Load (MPa)	Differential Reading	Next Load (MPa)	Differential Reading	Time to steady state (minutes)
0	8.73	200	40.00	2
200	41.80	0	9.73	4
0	9.32	200	42.60	2
0	9.64	250	48.63	1

Three cracks had been identified, though the signal from crack No.1 was swamping other indications that may have helped to locate other cracks.

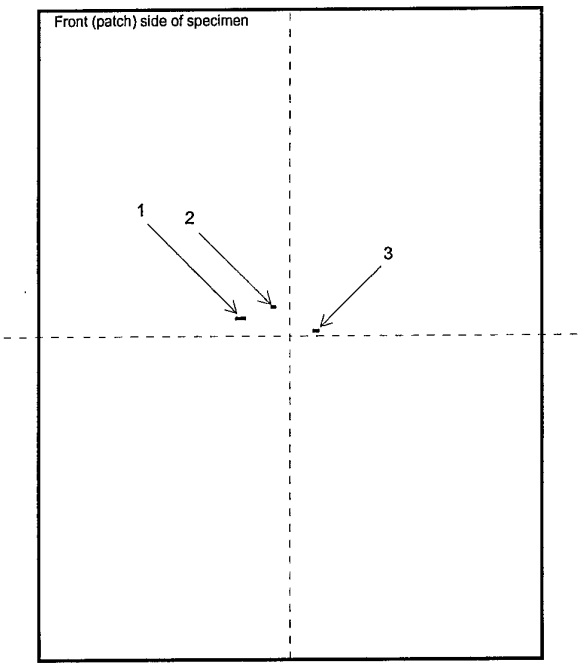

Figure 27: A schematic of the location of the three cracks detected by the structural integrity monitor (Model 2).

3.21 Program 29

3.21.1 Holographic Interferometry

The following table lists the holographic plates taken after the final program.

Table 16: Holographic plate test.

Plate No.	Exposure No.	Stress Min (MPa)	Stress Max (MPa)	Specimen Side	Exposure Time (seconds)
23	23	50	200	Rear	0.5/0.5
24	24	50	200	Rear	0.5/0.5
25	25	50	200	Front	0.5/0.5
26	26	50	200	Front	0.5/0.5
27	27	50	200	Front	0.5/0.5
28	28	50	200	Front	0.4/0.4
29	29	50	200	Front	0.3/0.3

Figure 28 is a schematic of the crack locations observed after program 29. Plate No. 24 clearly shows a number of cracks present, Figure 29.

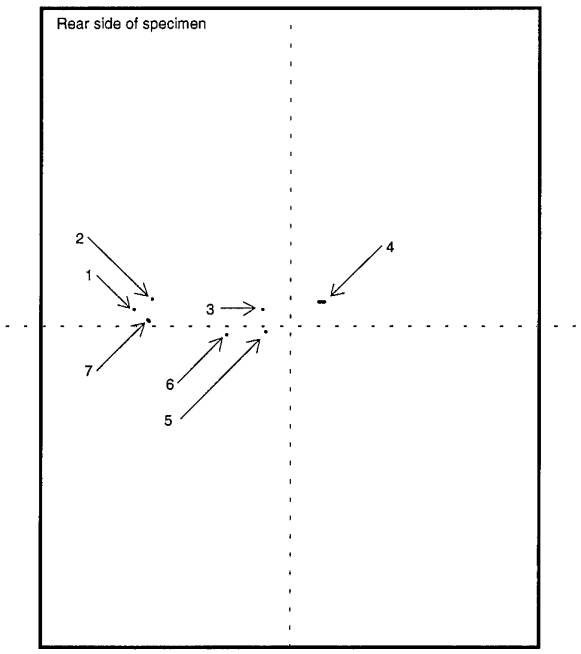

Figure 28: More cracks were located as shown in this schematic. Note that crack No.4 does not appear on this image.

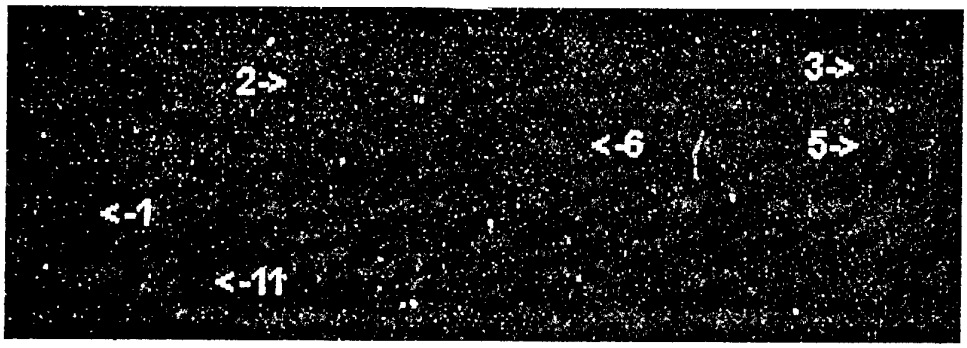

Figure 29: An image showing a number of the cracks. The larger the crack the more fringes that are distorted, from this cracks No. 1, No. 2 and No.3 are larger than crack No.5, No. 6 and No. 11. This is expected as cracks No.1, 2 and 3 were initially observed after program 26.

The structural integrity monitor patch was removed from the front of the specimen and a hologram taken of the specimen front. Figure 30 shows the location of the crack found by holographic interferometry, Figure 31. There are indications of three other cracks. The located crack is the main crack found by the structural integrity monitor.

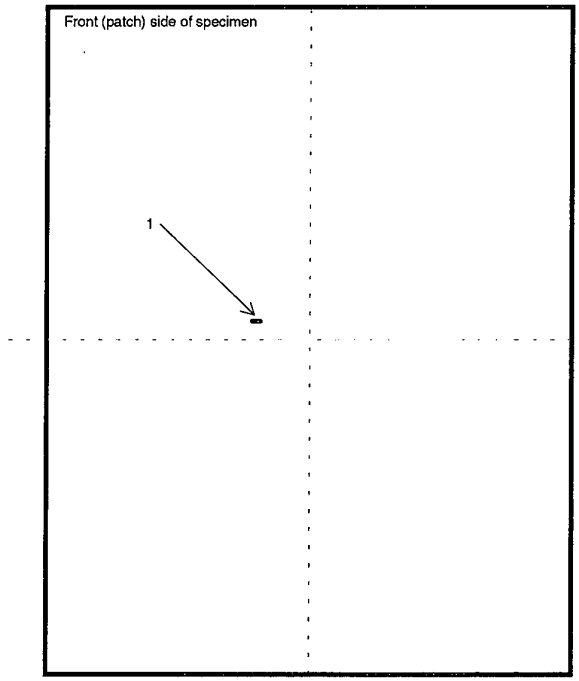

Figure 30: A schematic of the large crack located on the structural integrity monitor side after the patch was removed. The location agrees with the large crack found by the structural integrity monitor.

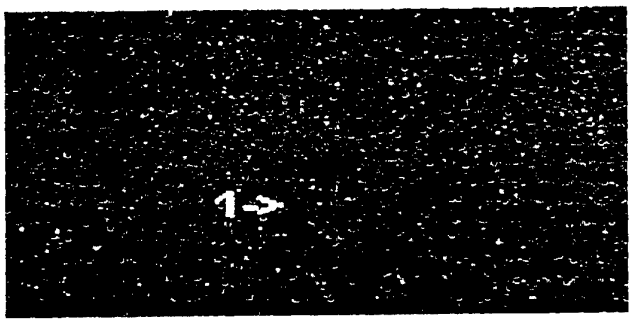

Figure 31: An image of the large crack located on the structural integrity monitor side of the specimen.

3.21.2 Structural integrity monitor

The differential reading jumped to a massive 83.60 (250 MPa), indicating the presence of a fast growing crack of significant size or the presence of numerous cracks. The monitor appears to be very sensitive to changes in crack length, once the crack has grown beyond the wall thickness.

Table 17: Structural integrity monitor results after program 29.

First Load (MPa)	Differential Reading	Next Load (MPa)	Differential Reading	Time to steady state (minutes)
0	9.32	Cyclic	22.58	
Cyclic	24.45	Cyclic	29.70	
0	10.06	200	74.00	2
0	10.46	250	83.60	1
250	83.60	0	9.31	3

3.21.3 Laser Ultrasonics

This inspection again showed indications of cracks at (i) and (ii). A final series of consistency checks were made on the data at this stage, including detailed comparison of the transmission results for various "y" values.

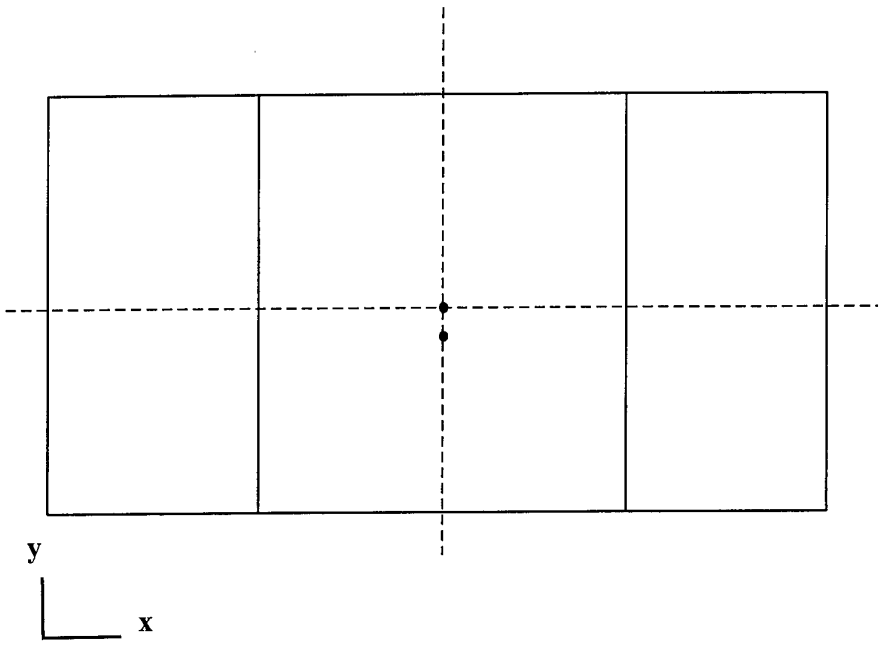

Figure 32: A schematic of the location of the two crack indications found with laser ultrasonics

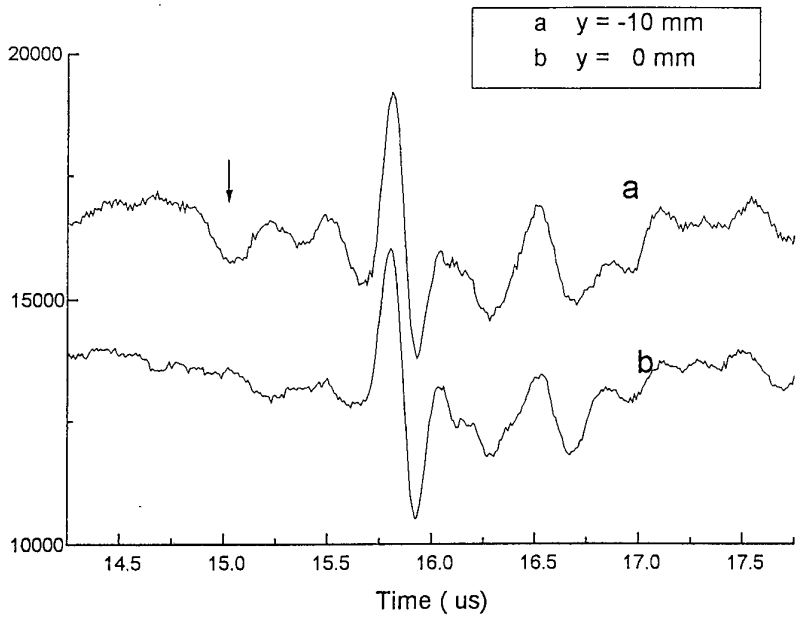

Figure 33: A typical waveform transmission from the test [3]. The difference between the two waveforms is the arrowed peak, which is attributed to a crack.

3.21.4 Dye penetrant

A fluorescent dye penetrant inspection was done to confirm the presence of any cracks. The specimen was loaded to 200 MPa and the dye swabbed onto the surface allowed to wick into the cracks for 2 hours and then excess dye was wiped carefully from the surface. Figure 35 and Figure 36 show the results from the dye penetrant inspection on reducing the load to zero, where the dye is squeezed back out of the cracks. The relative intensities of each indication was recorded since this could be correlated to crack size; the higher the intensity the larger the crack. Due to the low light intensities from the UV light source only the large cracks can be clearly seen on the video, figure 34.

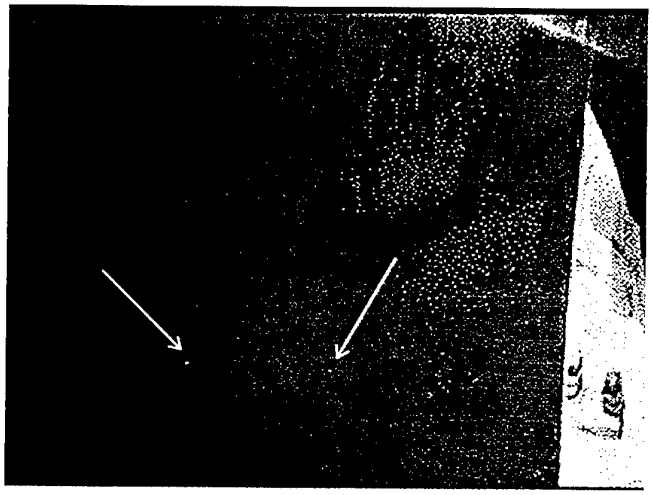

Figure 34: A photograph of the dye penetrant inspection. Note how only the two largest cracks had enough intensity to be recorded on the photograph.

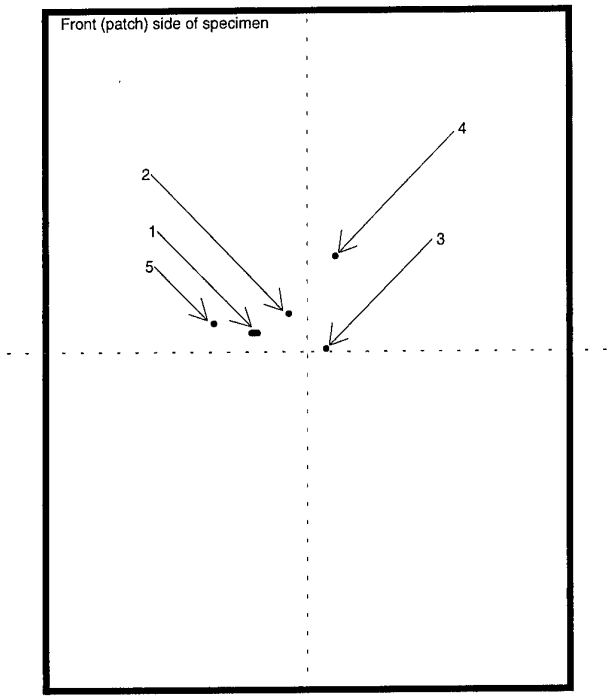

Figure 35: The five cracks located by fluorescent dye penetrant on the front of the specimen (structural integrity monitor side). The visual intensities are a good indication of the crack size and are as follows; crack 1-very bright, crack 2-bright, crack 3-bright, crack 4-weak and crack 5-weak

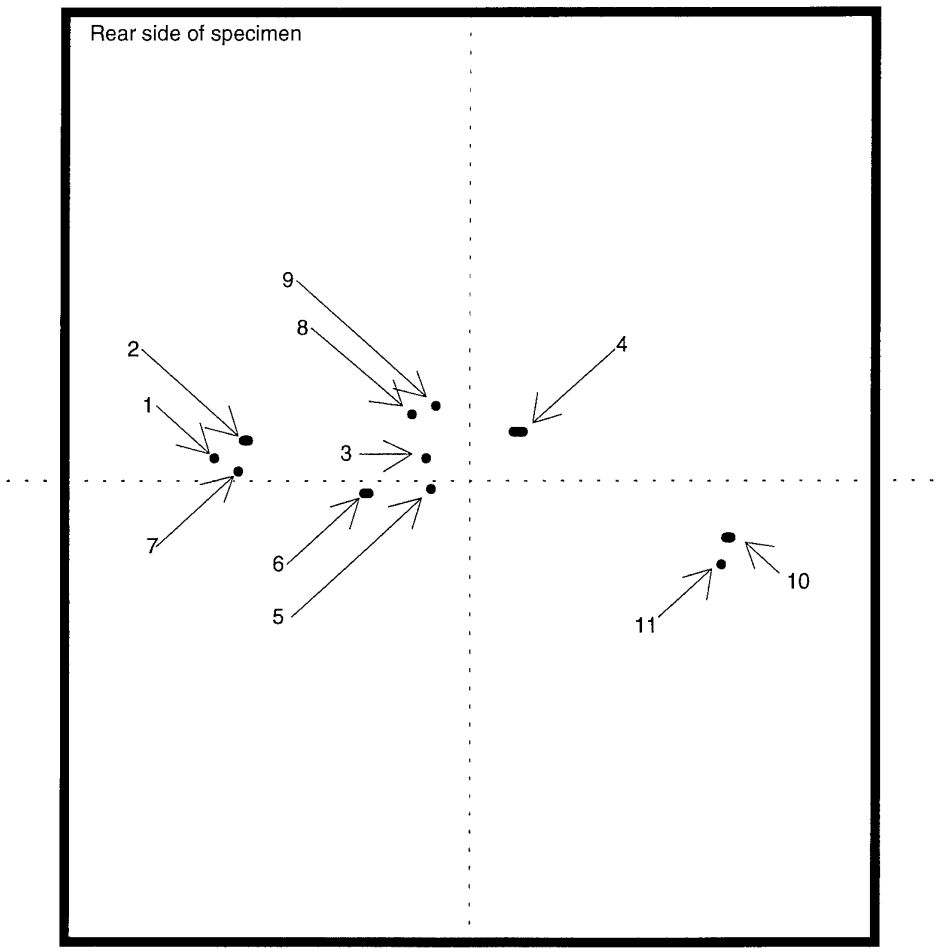

Figure 36: The eleven cracks found by fluorescent dye penetrant on the back of the specimen (holographic interferometry side). The visual intensities are a good indication of the crack size and are as follows; crack 4-very bright, cracks 2, 6, 10-bright and cracks 1,3,5,7,8,9,11-weak.

On a polished specimen the fluorescent dye penetrant is very sensitive and could be considered the best of the conventional NDI techniques used in this test.

3.21.5 Eddy current

The eddy current inspection was able to confirm the presence of the two large cracks F1-front of specimen and R4-rear of specimen. There were vague indications from F2, F3, R5, and R10, though the operators said they could not confirm them as cracks. The were no indications from the majority of cracks, F4, F5, R1, R2, R3, R6, R7, R8, R9, and R11.

3.21.6 Visual inspection

The microwatcher was able to locate the large crack on each face along with some of the medium sized cracks. Of the 16 cracks found by fluorescent dye penetrant only 6 could be found easily with the microwatcher. Images of the cracks taken from the video are shown in figure 37-figure 41.

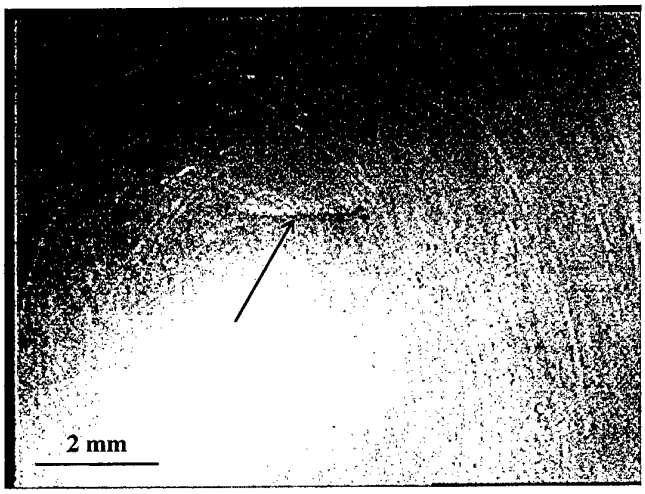

Figure 37: Images of the large crack on the "Davey System" side, observed with the microwatcher (crack No. F1).

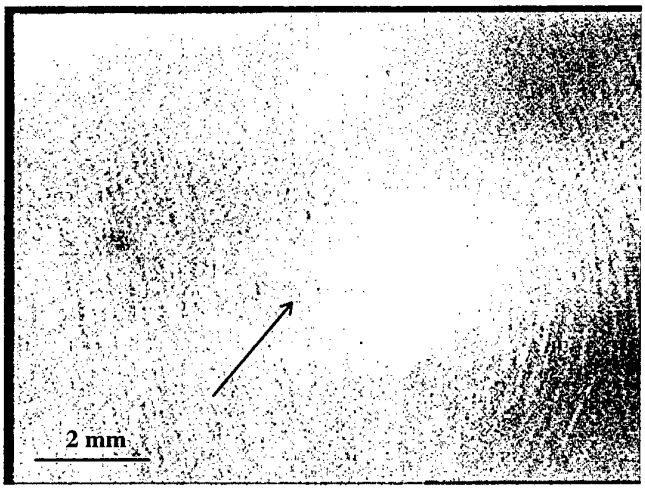

Figure 38: Images of the large crack on the holographic interferometry side, observed with the microwatcher (crack No. R4).

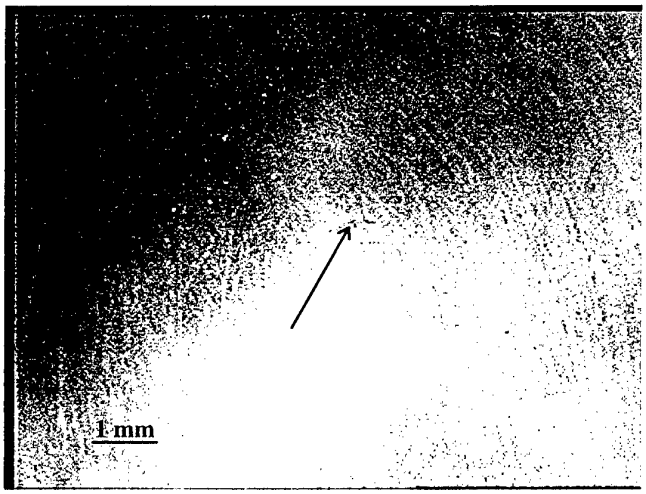

Figure 39: Images of the second crack on the holographic interferometry side, observed with the microwatcher (crack No. R6).

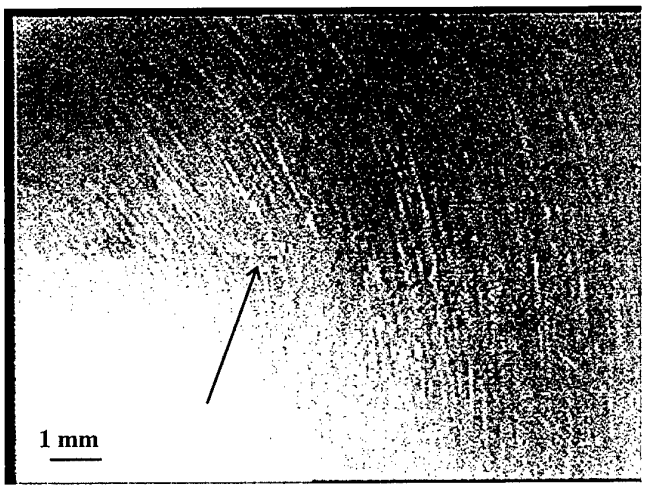

Figure 40: Images of the second crack on the "Davey System" side, observed with the microwatcher (crack No. F2).

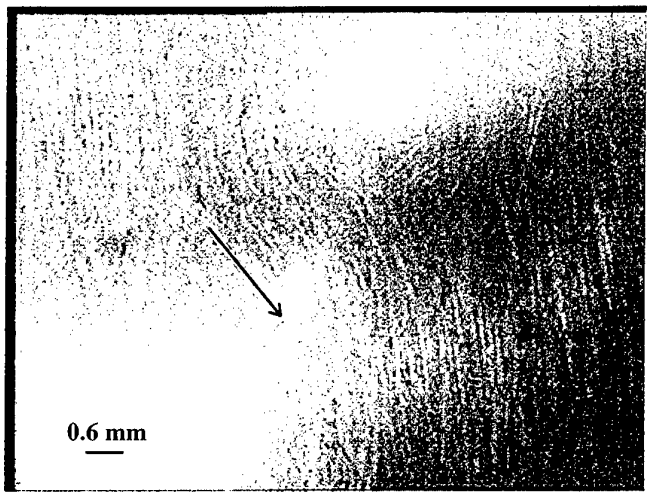

Figure 41: Images of the third crack on the Davey system side, observed with the microwatcher (crack No. F3).

4. Discussion

These large coupons under spectrum loading develop multi-site cracking. In this case there were 5 cracks in the front face and 11 cracks in the rear face. These cracks ranged in size from 2 mm down to 100 μm surface length. It would appear that a number of cracks initiated at approximately the same time but in each case one crack grew faster than the others. At this stage the coupon has not been broken open to confirm any of the crack depths.

4.1 Conventional NDI

Of the conventional NDI methods used to locate cracks on the polished specimen, fluorescent dye-penetrant was the most effective, indicating a large number and range of cracks. Dye penetrant detected 5 cracks on the front face ("Davey System") and 11 cracks on the back face (holographic interferometry and laser ultrasonics). The cracks detected by this method provided the comparison for all the other NDI methods.

The eddy current inspection was able to reliably detect the single large crack on each face (front and rear). There were possible indications from a number of other cracks (2 front face and 2 rear face), though the operators could not reliably confirm their presence. There were also a large number of small cracks not detected by eddy currents, 2 from the front face and 8 from the rear face.

The ultrasonic inspection also reliably detected the single large crack on each face, but could not reliably detect any of the other cracks.

A visual inspection using a microwatcher was able to locate four cracks, in particular the large crack (approx 2 mm) on each face.

4.2 Laser Ultrasonics

Laser ultrasonics initially detected four indications after program 14; at the time the cracks could not be confirmed by any other method, including use of a high powered microscope (mag =1000x). After program 25, two of the initial indications were confirmed as possible cracks and two of the indications as spurious signals generated by the test set-up. On completion of the test the two possible crack indications did not match any of the cracks located with the fluorescent dye penetrant inspection. This coupon geometry and technique do not facilitate accurate detection of small cracks. The spurious signals were due to difficulties in applying the technique, not only due to the 6-inch radius on which the cracking initiated but also because of other coupon faces which scattered ultrasonic waves over a wide range of angles.

4.3 Holographic Interferometry

Holographic interferometry initially detected three cracks after program 26, it then located another large crack after program 27 making a total of four cracks. This large crack was longer than the three cracks detected after program 26, but did not appear on the hologram taken after program 26. Another faint crack indication was observed in the hologram taken after program 28 and two more appeared in the hologram taken after program 29. This made a total of 7 crack indications by the completion of the test. Of these 7 crack indications, 5 could be found reliably in all the final holograms, and the other two could be observed in some of the holograms. The dye penetrant inspection revealed 11 cracks on this (the rear) face, though 3 of these indications were very faint.

A hologram of the front face also confirmed the presence of three cracks, one of which was large (approximately 2 mm long).

The continual improvements made to this method during the test, to produce greater reliability, make it difficult to assess over the trial period the efficiency of the complete system. The major problem with this method at present, is the interpretation of the holograms. Once the operator becomes familiar with what to look for, and how to look for it, the method is quite straightforward. Another problem is that a load must be applied to the component for this method to work; this may not be difficult to achieve but it adds another variable to be considered.

4.4 Structural Integrity Monitor

The initial Structural Integrity Monitor Model 1, was unsatisfactory for a number of reasons; firstly the sensor channel spacing was too large at approximately 1 mm, secondly the sensor pad was difficult to apply and lastly, it was difficult to precisely locate cracks. The Structural Integrity Monitor Model 2 was a substantial improvement over Model 1, with its LCD display, smaller sensor channels (approximately 250 μm) and adhesive backing; the overall system was now much more user-friendly.

The Structural Integrity Monitor initially detected possible cracking after 25 programs. After 26 programs three possible cracks could be located under the sensor pad. The system was able to highlight that one crack was growing faster than the other two cracks, and eventually swamped the signal from the two smaller cracks. Dye penetrants revealed five cracks on the front face, two of these cracks with very weak intensities. The two cracks with weak intensities were approximately 300 μm surface length which is near the detectability limit of the Structural Integrity Monitor. The Structural Integrity Monitor is particularly effective in that it can just be left in place with the system set-up to provide an audible alarm if the differential pressure exceeds certain limits. It was able to locate the cracks horizontally across the specimen but not vertically, though the system could possibly be adapted to also provide vertical location.

5. Conclusion

With the initial part of the test program completed a number of conclusions could be drawn. It is worth noting that the final aim of the work is to find a method that can reliably detect multi-site cracking (<1 mm) on peened surfaces. In this first phase, a polished specimen was initially used to determine the ability/reliability of each new method.

1. On polished specimens fluorescent dye penetrant provided the best method to locate cracks. However, this method has already been shown to be inappropriate for peened specimens, due to surface roughness effects.

2. Both the holographic interferometry method and the Structural Integrity Monitor were able to detect cracks not located by conventional methods such as eddy current and ultrasonics.

3. The holographic interferometry method was able to reliably detect 5 cracks with a possible 2 more crack indications, out of the 11 cracks located on the rear face.

4. Laser ultrasonics suffered from difficulties due to the geometry and size of the specimen and detected only 2 indications on the rear face (which contained 11 cracks). These indications did not correspond to cracks present at the end of the test. Two false positive indications were also obtained at the same time. The fact that no other indications were detected despite extensive crack development revealed by other methods, suggests that the two indications were also false positives.

5. The Structural Integrity Monitor was able to reliably locate 3 of the 5 cracks found on the front face. The other two cracks were found to be near the detection limit in size.

6. Both the holographic interferometry method and the Structural Integrity Monitor detected all cracks with a surface length greater than 1 mm (and possibly smaller for the holographic interferometry).

7. Both the holographic interferometry method and the Structural Integrity Monitor should work on peened surfaces because they are measuring a change rather than a direct reading.

6. Recommendations

Previous work at AMRL has already shown that conventional NDI techniques do not work reliably on rough peened surfaces. It is also unlikely that laser ultrasonics will work well on rough peened surfaces, however, it will be included in the next phase of testing to validate this theory.

Both the innovative NDI methods, Holographic Interferometry and Structural Integrity Monitor, have shown promise in their ability to detect multi-site cracking on polished surfaces. The next stage of the test program is to see if either method can detect multi-site cracking on a rough peened surface, similar to the F/A-18 488 bulkhead condition. In theory, because both methods are looking for a change rather than an absolute value they should work with peened surfaces, though whether the detectability limit and reliability will be the same has yet to be determined.

In the next stage large flat dogbone (25 mm across) specimens will be used, since they represent the flat bulkhead face that would need to be examined rather than the mould-line flange radius (6 inch). Each NDI method will have a peened dogbone specimen to detect cracks. When they detect a crack the specimen will be overloaded to confirm the presence of any crack. In this way a number of tests can be completed, checking both the detectability and reliability of each NDI method.

7. Acknowledgments

The authors would like to thank a number of people and organisations for providing their time and equipment. Ken Davey from Structural Monitoring Systems PTY LTD for the structural integrity monitor, Prof. John Baird and Bob Clark from ADFA for the initial holographic interferometry, Dr C. Scala and S. Bowles from SSMD for the laser ultrasonics. The authors would also like to thank Michael Ryan for running the test machine and Bruce Bishop, Howard Morton and Peter Virtue for the conventional NDI examinations.

8. Bibliography

1. Anderson, I. and Revill, G.,F/A-18 Fuselage Station 488 Free-Standing Bulkhead Fatigue Test, ARL-STRUC-TM-575, AR-006-111, November 1990

2. Barter, S.A., Athiniotis, N. and Lambrianidis, L., Examination of The Microstructure of 7050 Aluminium Alloy Samples, ARL-MAT-TM-403, AR-006-113, August 1990

3. C. Scala and S. Bowles, Laser Ultrasonic Results on large Polished Specimen, minute dated May 1996

4. Rumble, S.J., Introduction to Holographic Interferometry Applied to Strain Determination, ARL-STRUC-TM-443, AR-004-478, June 1986

5. Gordon, J., Lecture and Practical Session Notes on Holographic Interferometry, Run by AMRL for the Institute of Engineers Australasia course on "Experimental Stress Analysis", June 23-24 1994

6. Haraharan, P., Optical Holography Principles Techniques and Applications, First Edition, Cambridge University Press, 1984

7. Gordon, J. and Rowlands, D.E., An Improved Method of Investigation of Compressor Blade Fit Using Holographic Interferometry, ARL-STRUC-TM-577, January 1991

8. Instructions on Portable holographic system-ADFA

9. Davey, K., Operating manual for the Structural Integrity Monitor- Model 2

10. P.K. Sharp, N. Athiniotis, R. Byrnes, S. A. Barter, J. Q. Clayton and G. Clark, Assessment of RAAF F/A-18 FS488 Bulkhead Offcuts: Microstructure and Surface Condition, DSTO-TR-0326, June 1996

Appendix 1

Laser Interferometry Detection Method

Prof. John Baird
Department Of Mechanical Engineering
University College
The University of New South Wales
Australian Defence Force Academy
Canberra, ACT

Phone: (06) 268 8242
Fax: (06) 268 8276

The "Davey System"

Paul Kristensen
Managing Director
Structural Monitoring Systems PTY LTD
Level 21, 197 St George's Terrace
Perth 6000

Phone: (09) 481 0306
Fax: (09) 321 7154

Evaluation of Innovative NDI Methods for Detection of Widespread Fatigue Damage

P.Khan Sharp, D.E. Rowlands and G. Clark

DSTO-TR-0366

AUSTRALIA

1. DEFENCE ORGANISATION

a. Task sponsor ASI

b. S&T Program

Chief Defence Scientist
FAS Science Policy
AS Science Industry and External Relations
AS Science Corporate Management
} shared copy

Counsellor Defence Science, London (Doc Data Sheet)
Counsellor Defence Science, Washington (Doc Data Sheet)
Scientific Adviser to Thailand MRDC (Doc Data Sheet)
Senior Defence Scientific Adviser/Scientific Adviser Policy and Command (shared copy)
Navy Scientific Adviser (3 copies Doc Data Sheet and 1 copy distribution list)
Scientific Adviser - Army (Doc Data Sheet and distribution list only)
Air Force Scientific Adviser
Director Trials

Aeronautical and Maritime Research Laboratory
Director
Chief, AED
Dr A.A. Baker
Dr G. Clark
S. Lamb
P.K. Sharp
D. Rowlands

Electronics and Surveillance Research Laboratory
Director

DSTO Library
Library Fishermens Bend
Library Maribyrnong
Library DSTOS (2 copies)
Library, MOD, Pyrmont (Doc Data sheet only)
Australian Archives

c. Forces Executive
Director General Force Development (Sea) (Doc Data Sheet only)
Director General Force Development (Land)
Director General Force Development (Air)

d. Navy
No compulsory distribution

e. Army
ABCA Office, G-1-34, Russell Offices, Canberra (4 copies)

f. **Air Force**
OIC ASI (RAAF Williams)
OIC NDISL (RAAF Amberley)

g. **S&I Program**
Defence Intelligence Organisation
Library, Defence Signals Directorate (Doc Data Sheet only)

h. **Acquisition and Logistics Program**
No compulsory distribution

i. **B&M Program (libraries)**
OIC TRS, Defence Central Library
Officer in Charge, Document Exchange Centre (DEC), 1 copy
*US Defence Technical Information Centre, 2 copies
*UK Defence Research Information Centre, 2 copies
*Canada Defence Scientific Information Service, 1 copy
*NZ Defence Information Centre, 1 copy
National Library of Australia, 1 copy

2. **UNIVERSITIES AND COLLEGES**

Australian Defence Force Academy
Library
Head of Aerospace and Mechanical Engineering
Deakin University, Serials Section (M list), Deakin University Library, Geelong, 3217
Senior Librarian, Hargrave Library, Monash University
Librarian, Flinders University

3. **OTHER ORGANISATIONS**

NASA (Canberra)
AGPS
Paul Kristensen, Structural Monitoring Systems Pty Ltd, 20 copies

OUTSIDE AUSTRALIA

4. **ABSTRACTING AND INFORMATION ORGANISATIONS**
INSPEC: Acquisitions Section Institution of Electrical Engineers
Library, Chemical Abstracts Reference Service
Engineering Societies Library, US
American Society for Metals
Documents Librarian, The Center for Research Libraries, US

5. **INFORMATION EXCHANGE AGREEMENT PARTNERS**
Acquisitions Unit, Science Reference and Information Service, UK
Library - Exchange Desk, National Institute of Standards and Technology, US
National Aerospace Laboratory, Japan
National Aerospace Laboratory, Netherlands

SPARES (10 copies)

Total number of copies: 79

DEFENCE SCIENCE AND TECHNOLOGY ORGANISATION
DOCUMENT CONTROL DATA

1. PRIVACY MARKING/CAVEAT (OF DOCUMENT)

2. TITLE

Evaluation of innovative NDI methods for Detection of Widespread Fatigue Damage

3. SECURITY CLASSIFICATION (FOR UNCLASSIFIED REPORTS THAT ARE LIMITED RELEASE USE (L) NEXT TO DOCUMENT CLASSIFICATION)

Document	(U)
Title	(U)
Abstract	(U)

4. AUTHOR(S)

P. Khan Sharp, D.E. Rowlands, and G. Clark

5. CORPORATE AUTHOR

Aeronautical and Maritime Research Laboratory
PO Box 4331
Melbourne Vic 3001

6a. DSTO NUMBER	6b. AR NUMBER	6c. TYPE OF REPORT	7. DOCUMENT DATE
DSTO-TR-0366	AR-009-749	Technical Report	August 1996

8. FILE NUMBER	9. TASK NUMBER	10. TASK SPONSOR	11. NO. OF PAGES	12. NO. OF REFERENCES
M1/8/929	95/089	ASI	53	8

13. DOWNGRADING/DELIMITING INSTRUCTIONS

None

14. RELEASE AUTHORITY

Chief, Airframes and Engines Division

15. SECONDARY RELEASE STATEMENT OF THIS DOCUMENT

Approved for public release.

OVERSEAS ENQUIRIES OUTSIDE STATED LIMITATIONS SHOULD BE REFERRED THROUGH DOCUMENT EXCHANGE CENTRE, DIS NETWORK OFFICE, DEPT OF DEFENCE, CAMPBELL PARK OFFICES, CANBERRA ACT 2600

16. DELIBERATE ANNOUNCEMENT

No limitations.

17. CASUAL ANNOUNCEMENT Yes

18. DEFTEST DESCRIPTORS

Non-destructuive investigation, widespread damage, fatigue, aluminium, holography, Davey System

19. ABSTRACT

High-performance high-strength aircraft components such as the F/A-18 FS488 bulkhead can experience catastrophic failure in fatigue tests from very small cracks. At the same time, the efficiency of design methods used for these components results in highly uniform stressing, and a large number of fatigue cracks all growing at approximately the same rate - multi-site cracking. These circumstances place extreme demands upon the use of Non-Destructive Inspection (NDI) methods for finding and characterising defects, and when surface treatments such as peening are also employed to extend service fatigue life, it becomes almost impossible to detect the small crack arrays which are of concern. This report examines and evaluates some novel Non-Destructive Inspection techniques, that may allow numerous small cracks (less than 1 mm) over a large area to be detected. Conventional NDI techniques are also used for comparative purposes.

The novel techniques used are 1) Holographic Interferometry, 2) Structural Integrity Monitor, and 3) Laser Ultrasonics. This report examines the extent to which each technique can locate cracks on a large polished specimen representing part of a bulkhead. Techniques which perform well in this evaluation will be further evaluated on a large peened specimen.